DETECTION OF BONE MARROW STEM CELL DIFFERENTIATION WITH MAGNETIC LEVITATION

A Thesis Submitted to
the Graduate School of Engineering and Sciences of
İzmir Institute of Technology
in Partial Fulfillment of the Requirements for the Degree of

MASTER OF SCIENCE

in Bioengineering

by
Öykü SARIGİL

July 2019
İZMİR

We approve the thesis of **Öykü SARIGİL**

Examining Committee Members:

_____
Assoc. Prof. Dr. Engin ÖZÇİVİCİ
Department of Bioengineering, İzmir Institute of Technology

_____
Asst. Prof. Dr. Hüseyin Cumhur TEKİN
Department of Bioengineering, İzmir Institute of Technology

_____
Asst. Prof. Dr. Hümeyra TAŞKENT SEZGİN
Department of Genetics and Bioengineering, İzmir University of Economics

16 July 2019

_____
Assoc. Prof. Dr. Engin ÖZÇİVİCİ
Supervisor, Department of Bioengineering

_____
Prof. Dr. Erdal BEDİR
Head of the Department of
Bioengineering

_____
Prof. Dr. Aysun SOFUOĞLU
Dean of the Graduate School of
Engineering and Sciences

ACKNOWLEDGMENTS

Firstly, I would like to express my sincere appreciation to my supervisor Assoc. Prof. Dr. Engin ÖZÇİVİCİ for all of the guidance, encouragement, patience, support throughout my graduate education. The opportunities which he provided for me over two years are very valuable and the reason to beginning of my academic career. I would like to thank Asst. Prof. Dr. Hüseyin Cumhur TEKİN, Assoc. Prof. Dr. Gülistan MEŞE ÖZÇİVİCİ and Assoc. Prof. Dr. Özden YALÇIN ÖZUYSAL for their mentorships throughout my thesis study. I thank Sena Yaman for fabricating the magnetic levitation device and Esra YILMAZ for simulation of magnetic field distribution in levitation device. I would also like to thank Müge ANIL İNEVİ for her all technical training, help and support during my laboratory experiments, as well as, her moral support for my apprehension and personal matters. I came to know about so many things by her training. In addition, I would like to acknowledge 215S862 project supported by The Scientific and Technological Research Council of Turkey (TÜBİTAK).

I am very thankful to Ekin KESTEVUR DOĞRU and Eyüp BİLGİ for their worthwhile advices for my study and conversation on any topics. I am so grateful to know they are the friends that I can always ask for help. Also, I would like to thank to all my office colleagues, especially Gamze DOĞAN, Yağmur Ceren ÜNAL, and my dear friends Hilal Deniz YILMAZ, Meltem GÜZELGÜLGEN, Sami ŞANLIDAĞ, Defne Deniz DİNÇ, Büşra DAYIOĞLU and Canset NALÇACI, who I got to know during my undergraduate education, for their friendships and supports. Moreover, I would like to express my special thanks to dear Yiğit Ege ÇÖMLEKÇİ for all support and encouragement with his warm-hearted personality.

I owe debt of gratitude to my dear mother Şükran TANYEL for her endless support, always being by my side, teaching me being strong and how to cope with difficulties and to my sister Ezgi SARIGİL for her loving support.

I would not get where I was without all these people. Therefore, I would like to express my sincere thanks to everyone.

ABSTRACT

DETECTION OF BONE MARROW STEM CELL DIFFERENTIATION WITH MAGNETIC LEVITATION

Adipocytes are the major energy depots which primarily compose adipose tissue in the body. They are mainly responsible for energy balance and also play a crucial role as endocrine and paracrine cells. Hypertrophy (cell size increase) and hyperplasia (cell number increase) are two mechanisms for adipose tissue growing, relating to some diseases such as obesity, osteoporosis, diabetes and anorexia nervosa. In this context, to detect and identify adipocytes has become critical to determine increase in cell size and cell number, thereby, it facilitates to understand mechanisms and process of adipocyte differentiation and provide to develop therapeutic strategies for the treatment and prevention of obesity and obesity-related diseases. Traditional or advanced techniques used for adipocyte detection and examination are available with their accomplished applications. However, they have some restrictions on adipocyte detection, such as being complicated and expensive operations or causing cell defects. Magnetic levitation is a novel technique with the capability of label-free, density-based detection using the principle of movement of the cells to lower magnetic field region in a paramagnetic medium. In this study, we used magnetic levitation system for detection of adipogenic-differentiated cells in heterogeneous cell populations. Results showed that levitation platform could detect the changes in lipid content of mesenchymal stem cells during adipogenic differentiation. This microfluidic system has a promising future with modification to sort adipogenic cells.

ÖZET

KEMİK İLİĞİ KÖK HÜCRE FARKLILAŞMASININ MANYETİK KALDIRMA İLE TESPİTİ

Adipositler vücuttaki adipoz dokuyu oluşturan ana hücrelerdir. Temel görevleri enerji dengesini sağlamak olan bu hücreler, aynı zamanda önemli endokrin ve parakrin fonksiyon gösterirler. Adipoz doku, hiperplazi (hücre sayısında artış) ve hipertropi (hücre boyutunda artış) olmak üzere iki farklı mekanizma ile büyümektedir. Bu iki mekanizma adipojenez sırasındaki anormallikleri tanımlamada önemli parametrelerdir. Adipositlerin tespiti ve mekanizmalarının tanımlanması başta obezite, osteoporoz, diyabet olmak üzere pek çok ilişkili hastalıkların tedavisi için terapötik stratejilerin gelişiminde önemli bir basamaktır. Adiposit tespiti için kullanılan geleneksel veya gelişmiş teknikler başarılı uygulamalarına rağmen pahalı ve zor yöntemler olmaları veya çalışma sırasında hassas adiposit hücrelerinde hasara sebep olmaları gibi bazı kısıtlamalara sahiptirler. Hücrelerin paramanyetik bir ortamda düşük manyetik alana yönelmesi prensibine dayanan manyetik levitasyon sistemi, hücreleri etiketlemeden, yoğunluklarına bağlı olarak ayırt etme olanağı sağlayan yeni bir tekniktir. Bu çalışmada, heterojen bir popülasyondaki adipojenik hücrelerin tespiti için manyetik levitasyon sistemi kullanılmıştır. Sonuçlar, kök hücrelerin adipojenik farklılaşma sürecinde değişen lipit içeriği aracılığıyla adipojenik hücrelerin tespitinin manyetik levitasyon yöntemi ile münkün olduğunu göstermektedir. Ayrıca, mikroakışkan özellliği ile bu sistem, tespiti yapılan adipositlerin ileri çalışmalarda kullanılmak üzere ayrımına da olanak sağlama potansiyeline sahiptir.

TABLE OF CONTENTS

LIST OF FIGURES

Figure **Page**

Figure **Page**

CHAPTER 1

INTRODUCTION

1.1. Adipocytes and Adipose Tissue

Adipose tissue is one of the most complex tissue composed of mature adipocytes (> 90%) as well as stromal vascular fraction, which consists of preadipocytes, fibroblasts, endothelial cells, vascular smooth muscle cells, immune cells, and adipose stromal cells (adipose-derived stem cells) [1]. Adipocytes, also known as fat cells, are the main component of adipose tissue, and they mainly control energy balance by storing and mobilizing triglycerides in the body [2]. Besides the regulation of energy balance and homeostasis, they provide mechanical support for internal organs and present essential endocrine and paracrine functions [2, 3]. Several chemokines, cytokines and hormones are secreted by adipocytes, regulating many physiological activities such as glucose homeostasis, immune response, angiogenesis [4-6].

There are typically three adipocyte types; white, brown and beige adipocytes [7, 8]. White adipocytes are the predominant type in human and characterized with one big lipid droplet, peripheral nucleus and few mitochondria [6, 9]. They constitute the majority of adipocytes in body and they are responsible for energy storage and mechanical support. On the other hand, brown adipocytes compose of numerous small lipid droplets, many mitochondria and nucleus found in center [9]. Brown adipocytes are mainly found in human newborns and their primary function is adaptive thermogenesis regarding to abundant mitochondria [6-8, 10, 11]. Beige adipocytes are other thermogenic adipocytes. Like brown adipocytes, they control energy homeostasis in the body [12]. However, these adipocyte types, as well as white adipocytes, show the difference in their origin, gene expression, and function [13].

Adipocytes are characterized by internal lipid droplets (~90% of cell volume) and during adipogenesis cell volume increases [2, 14]. Therefore, adipocyte size varies from 20 μm to 250 μm to adapt themselves to store lipid droplets [9, 14, 15]. Adipose tissue grows by two mechanisms called as hyperplasia and hypertrophy, and the process affects the

cellular metabolism [11, 16]. Hyperplasia refers to increasing in cell number, and hypertropy is the increasing in cell size. In these two possible growth mechanisms, adipocytes show different biological properties (Figure 1). Hyperplasic growth is related to beneficial phenomena such as decreased basal fatty acids (FFA) release, immune cell recruitment, hypoxia, pro-inflammatory cytokine release, fibrosis, and increased adiponectin and insulin sensitivity. However, hypertrophic growth is linked to harmful phenomena, such as increased basal fatty acids release, immune cell recruitment, hypoxia, pro-inflammatory cytokine release, fibrosis, decreased adiponectin, and impaired insulin sensitivity [11]. These two mechanisms are important parameters to describe abnormalities in adipogenic differentiation that leads to relevant diseases, such as obesity. Adipocytes are primarily found in the visceral adipose tissue located around internal organs, such as stomach, liver, and subcutaneous adipose tissues located under the skin [17-19]. Besides, they are also found in bone marrow adipose tissue [20, 21].

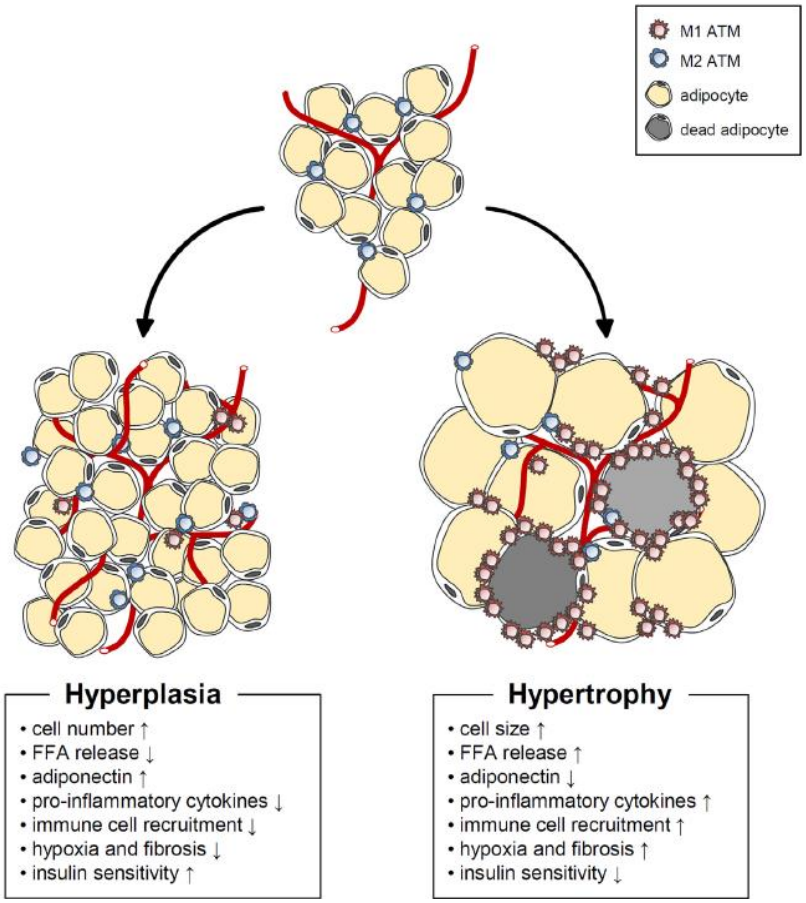

Figure 1. Growth mechanisms of adipose tissue (Source: Choe et.al,2016) [11]

1.2. Marrow Adipocytes and Adipogenic Differentiation in Bone Marrow

Bone marrow consists of red marrow including mainly hematopoietic cells, and yellow marrow containing highly adipocytes, which give the color to yellow marrow. Red marrow, which mainly fills the bone cavity at birth, is replaced by yellow marrow with ageing (Figure 2) [22, 23]. Bone marrow adipose tissue (BMAT) results from accumulation of adipocytes, which contain a big lipid vacuole, within bone marrow and BMAT shows different characteristics by comparison with white and brown adipose tissue [22, 24]. For example, bone marrow adipocytes (BMAs) present similar morphology to white adipocytes, while they express gene markers of brown adipocytes [25, 26].

It was previously described that there are two types of marrow adipose tissue (MAT), showing physiological and morphological differences [27, 28]. They are called as regulated MAT (rMAT) and constitutive MAT (cMAT) which present within red marrow and yellow marrow, respectively [27]. Adipocytes compose 45% of red marrow whereas they are up to 90% in yellow marrow. rMAT adipocytes are smaller in size (32.5 ± 2.4 μm diameter) than cMAT adipocytes (37.8 ± 1.2 μm diameter) [27]. Also, rMAT and cMAT adipocytes differ in some regulations of adipocyte marker genes[25, 27].

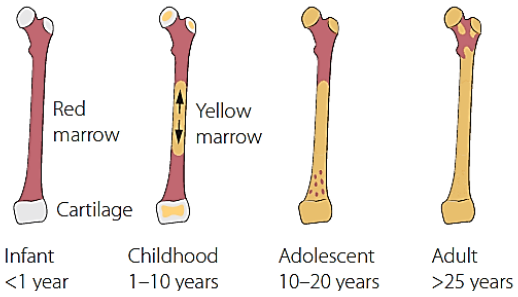

Figure 2. Conversion of haematopoietic to adipose marrow in bone (Source: Veldhuis-Vlug and Rosen, 2018) [23]

Bone marrow adipocytes (BMAs) are derived from mesenchymal stem cells which can also differentiate into osteoblasts [29]. Cell lineage commitment in bone marrow is stimulated by adipogenic and osteogenic factors. Numerous factors committed to

adipocytes themselves and neighboring cells are important during adipogenesis in bone marrow [29]. Like to be regulated adipogenesis by surrounding cells, BMAs also have an important role on bone marrow homeostasis by regulating endocrine and paracrine factors related to osteogenesis [27]. In previous studies, it was shown that marrow adipocytes inhibit osteoblastogenesis which is concomitant to bone formation by osteoblasts, whereas promotes osteoclastogenesis with regard to bone resorption by osteoclasts [27, 30]. Differentiation of stem cells can be influenced by various factors (Figure 3) [29, 31-34]. The balance between osteogenesis and adipogenesis has a crucial role on bone health. For example, absence of mechanical load on stem cells causes to shift to adipogenesis and result in bone loss in astronauts [35, 36]. In the literature, it has been indicated that bone adiposity was associated with osteoporosis, osteopenia and other conditions caused to bone loss, such as increased cortisol production, glucocorticoid treatment, ageing [37, 38]. Besides to relation of BMAs with bone remodelling, they are in touch haematopoietic microenvironment. Previously, in some studies, it was shown that BMAs inhibit haematopoiesis by repressing growth and differentiation of haematopoietic stem cells [39]. However, recently, it was seen that hematopoietic regeneration was promoted by marrow adipocytes [40]. Also, there are some studies which suggest that marrow adipocytes influence bone metastasis because they provide energy source and release secretion factors which can inhibit or promote bone metastasis [41, 42].

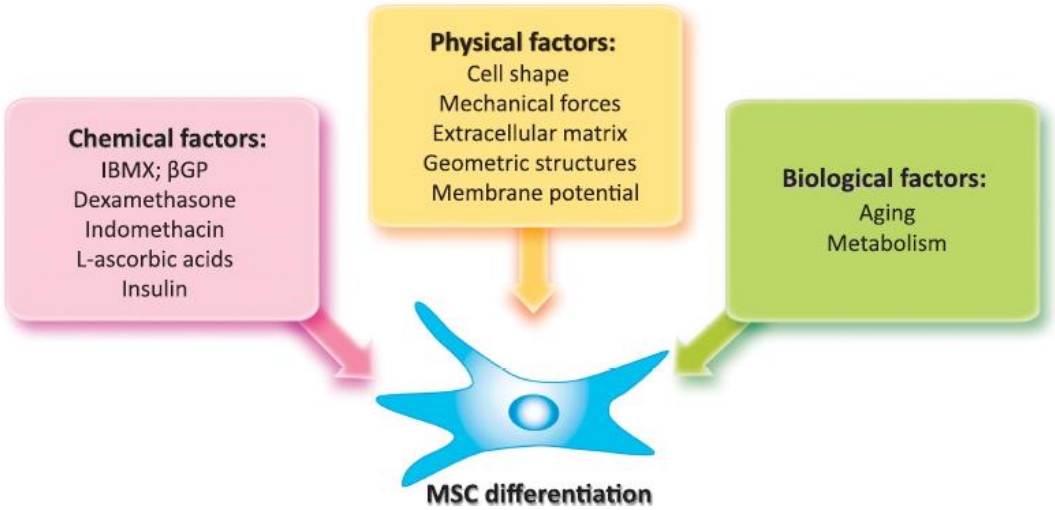

Figure 3. Control of the balance between osteogenic and adipogenic differentiation of mesenchymal stem cells by chemical, physical, and biological factors (Source: Chen et. al.,2016) [29]

1.3. Adipocyte Detection Techniques and Density-based Detection of the Cells

Relation between adipocytes and obesity and obesity-related diseases is the main reason of interest in studies for determination of morphology and physiology of adipocytes. Proper determination of adipocyte characteristics requires detection of adipocytes based on molecular or cellular parameters. Identification of adipocytes can be followed by proper biomedical application, *in vitro* or *in vivo*, to test the desired hypothesis.

Increased intracellular lipid droplets (hyperplasia) and cellular volume (hypertrophy) are key aspects of adipogenic differentiation. The conventional method to visualize adipocytes is optical microscopy by staining the cells with lipophilic dyes (e.g. Oil-Red-O, Nile Red, Bodipy 493/503 and Sudan III) [43-46]. Optical microscopic techniques for adipocyte detection is considerable useful due to being simple, however, they generally produce semi-quantitative results. Also adipogenic differentiation can be identified by detection of adipogenic marker proteins such as P107, that control the fate of differentiated adipocytes in stem cells or progenitor cells [47], or by quantitation of adipogenic marker genes such as proliferator-activated receptor gamma (PPARγ), CCAAT-enhancer binding protein α (C/EBPα), adipocyte determination and differentiation factor 1 (ADD1), adipocyte P2 (aP2) by real-time PCR [23, 32, 48, 49]. Nevertheless, these techniques are labour-intensive, take long time during process and more importantly, they eliminate the potential of the recovery of cells for further studies.

In addition to conventional techniques, some of advanced techniques, such as flow cytometry, can also be used for adipocytes detection [47]. However, utilization of nozzles in the flow-cytometry system restricts the application of this technique for mature adipocyte detection due to fragile and large structure of mature adipocytes [50, 51]. Other alternatives for adipocyte detection/separation are based on labelling of the cells with fluorescent or magnetic labels or microfluidic platforms which need liquids with different densities to separate the cells [52-57]. Also, there are various techniques which perform cell detection as label-free. These techniques, included electric cell-substrate impedance sensing (ECIS) systems which allow determining impedance changes in cells or Coherent anti-Stokes Raman scattering (CARS) imaging, require complex and expensive instrumentation and cannot enable to detect the cells in single-cell level [58-61].

Single cell density changes during some physiological events such as apoptosis, cell cycle, disease states as well as cell differentiation [57, 62-65]. Therefore, the single-cell density phenotype can be used as an indicator of cell state and it can be utilized to distinguish cell populations. Density gradient centrifugation is a widely accepted method to measure the average density of a cell population [66, 67]. It relies on moving of cells to their isopycnic point in density gradient. However, the solutions used for creating a density gradient can negatively affect the cell density and viability during long prosessing time with high centrifugal forces [57, 68]. Besides, the dynamic range and resolution of the system are inversely related, resulting in loss of resolution when high dynamic range is required [57]. Some microfluidic systems, such as suspended microchannel resonator (SMR) system and optically induced electrokinetics (OEK) microfluidic platform, enable density measurements on single cells whereas density gradient centrifugation method provides an average density for cell population [57, 69-71]. SMR is a microfluidic mass sensor consisting of cantilever which oscillates proportional to the buoyant mass of the cells during cell passing in two fluids with different densities. SMR system is highly precise in measuring cell density in single cell level, however, it is very time-consuming because of requiring passage of each cell through the cantilever, and it requires different carrier fluid density based on application. OEK platform is recently demonstrated method of measuring single cell density with princible of combining sedimentation principle and optically induced electrokinetics technology. This system has a complicated fabrication with optical elements and virtual electrode setups. Another alternative for measuring of single-cell density is the magnetic levitation, which is novel technology depending on movement of cells to the lower magnetic field region in a paramagnetic medium and position according to their density. This system provides label-free, real-time monitoring for density measurement of single cells within short time process.

1.4. Magnetic Levitation

Magnetic levitation is a physical method for density measurement of cells or materials. The principle of the magnetic levitation technique bases on movement of diamagnetic or weakly paramagnetic objects from higher magnetic field region to lower magnetic field region in the presence of applied magnetic field.

1.4.1. Magnetism of Objects

Magnetism is a physical phenomenon that is produced by the orbital motion of electrons and spin moments [72]. All matters exhibit magnetic property due to magnetic field produced by electrons orbiting the nucleus. Magnetism is classified into five major groups; diamagnetism, paramagnetism, ferromagnetism, antiferromagnetism and ferrimagnetism, according to behaviour of electrons in a magnetic field [73]. The most common types of magnetism are diamagnetism, paramagnetism, ferromagnetism. Diamagnetic substances consist of atoms of which net magnetic moments are zero because they have no unpaired electrons [72, 74]. However, in the presence of external magnetic field applied to diamagnetic substances, it is induced a weak magnetic dipole moment in the opposite direction to the applied magnetic field and diamagnetic substances are weakly repelled [74]. Diamagnetic property is presented in all materials and some materials such as gold, silver, silicon only display diamagnetism [75]. Diamagnetic materials have negative magnetic susceptibility ($\chi<0$), which is a measure of which matters become magnetized, and it does not change with temperature in diamagnetic materials [74, 76]. Paramagnetism results from unpaired electrons in partially filled orbitals in matters, therefore, they have a net magnetic moment [76, 77]. The magnetic moment can be quite larger in materials which have many unpaired electrons, such as lanthanite metals. In the presence of an external magnetic field, paramagnetic materials are temporarily magnetized in the same direction of applied magnetic field and attracted by the magnetic field. Paramagnetic materials have small positive magnetic susceptibility ($\chi>0$) and they are relatively dependent on temperature [76]. On the other hand, ferromagnetic materials are magnetized easily and attracted by magnets. Ferromagnetic susceptibility is much greater than paramagnetic and diamagnetic susceptibility and it varies with magnetic field [76]. Iron, nickel, cobalt, which are the most common ferromagnetic substances, and ruthenium are only ferromagnetic elements at room temperature [78]. The most of ferromagnetic materials lose their ferromagnetic properties above their Curie temperature and they present paramagnetic property [76]. For example, gadolinium, which is the fourth discovered ferromagnetic element, is paramagnetic above 20 °C [76, 79]. Ferromagnetism is used to create permanent magnets [73]. Neodymium magnets (known as NdFeB) are permanent magnets made from an alloy of neodymium, iron, and boron. These magnets are commercially the strongest permanent magnets. By changing

in their alloy composition, manufacturing technique and microstructure, neodymium magnets can present various magnetic properties by differences at resistance to demagnetization, strength of magnetic field output, temperature coefficients and operating temperature [80]. There are different grades of neodymium magnets, ranging from N24 to N52. Among them, N52 grade neodymium provides high magnetic performance.

1.4.2. Magnetic Liquids

Several magnetic liquids which show differences in terms of their magnetic susceptibility can be used for magnetic levitation. In previous studies, ferrofluids and paramagnetic salt solutions were used for different applications such as cell manipulation and separation, trapping [81-84]. Ferrofluids are colloidal suspensions which consist of very small magnetic particles, such as magnetite (Fe_3O_4), with diameter of around 5-20 nm [81, 85]. The nanoparticles are covered by surfactants to keep them stable in suspension [86]. They have relatively high magnetic susceptibility and magnetization and their susceptibility can be controlled by concentration of magnetic particles in the carrier fluid [87]. Another type of magnetic liquids is paramagnetic salt solutions. These solutions are composed of paramagnetic metals and chelating agents or halides [87]. They have lower magnetic susceptibility compared to ferrofluids. Similarly to ferrofluids, paramagnetic salt solutions can also be manipulated in terms of their susceptibility in the solution by changing their concentration. Paramagnetic salt solutions are regarded as to be more suitable for density measurement applications because of the fact that the stronger magnetic properties are not required for these applications whereas ferrofluids are proper for microfluidic systems with continued flow, such as pumping, mixing or sorting systems [85, 88]. There are different types of paramagnetic salt solutions available. For example, gadolinium(III) chloride ($GdCl_3$) and manganese(II) chloride ($MnCl_2$) are widely used in levitation of objects due to advantage of transparent forms and high susceptibilities [89]. $GdCl_3$ has higher magnetic susceptibility than $MnCl_2$ due to 7 unpaired electrons of gadolinium(III) [90]. However, higher concentrations of these paramagnetic agents might cause a toxic effect on living cells. In the previous studies, concentration of paramagnetic salt solutions has been used between the range of 0.1-1 M to prevent negative effects and exhibit biocompatibility [87]. In addition to using appropriate concentration of

paramagnetic solutions, another alternative way to improve biocompatibility is to use chelated forms of paramagnetic agents. Several types of approved gadolinium-based agents are used for magnetic resonance imaging [91]. Gadolinium-based agents are classified by their overall charge and ligand framework (ionic, non-ionic, linear and macrocyclic) [92]. The macrocyclic structures are more stable than linear forms and make difficult to release free ion in solution [93]. Gadobutrol, which has non-ionic and macrocyclic structure composed of gadolinium (Gd^{3+}) chelated with butrol (Figure 4), is a paramagnetic medium which get recently interest for magnetic levitation of living cells due to its high biocompatibility [94-98].

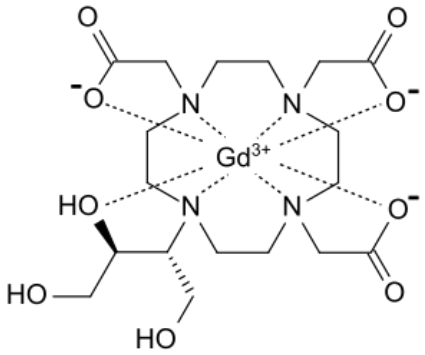

Figure 4. Molecular structure of gadolinium contrast agent, Gadobutrol (Gadavist) (Source: Trog et. al.,2019) [96]

1.4.3. Magnetic Levitation System and Its Applications

Magnetic levitation is a method based on using magnetic field to levitate diamagnetic samples according to their density [84, 99]. When diamagnetic substances such as, water, minerals, proteins, DNA, as well as most of the cell types, are placed in magnetic field, they acquire a net magnetic moment in the opposite direction to the magnetic field as a result of the rearrangement of the spin and orbital motions of their electrons and they are slightly repelled by external magnetic fields [100-104]. However, a simple way to increase response of diamagnetic substances to applied magnetic field is to use paramagnetic liquids which have larger magnetic susceptibility than diamagnetic

substances [89, 99]. With attraction of paramagnetic liquids by magnetic field, diamagnetic substances act as magnetic holes and move to weaker magnetic field region [74, 81].

Magnetic levitation can be performed by two ways termed as positive magnetophoresis and negative magnetophoresis [105]. Positive magnetophoresis is a technique that is based on labeling of the cells with magnetic beads. Thereby, the magnetically labelled samples move to higher magnetic field region and non-magnetic and magnetic samples are separated [106]. Positive magnetophoresis was previously used in separation of different cell types, such as blood cells and cancer cells. Also, it was demonstrated the technique enables to 3D culture of cells [107]. However, additional steps for labeling are required during this technique and it is time-consuming. On the other hand, negative magnetophoresis, which was also used in this study, is a novel technique that is in spotlight because it is label-free and mimics weightlessness environment. Applicability of negative magnetophoresis technique to studies which positive magnetophoresis was used has been shown in different researches. Similarly to positive magnetophoresis applications, negative magnetophoresis has been used for density measurement, cell separation, sorting, 3D biofabrication [82, 108-112]. Previously, magnetic levitation system which simulates weightlessness environment has been performed to study the effect of space microgravity on morphology and physiology of the cells [113, 114]. By using various cell types, such as yeast and bacteria, changes in cell growth, cell cycle, transcriptional profile were determined [113-115]. Also, continuous flow was applied to living cells and cell sorting based on their size was presented [90, 116]. The potential of the levitation system as 3D biofabrication tool was shown by 3D assembly of different cell types (stem cells, cancer cells, blood cells [109-111, 117]. The manipulations of the cells by magnetic levitation system can be performed by changing the magnet shape or configuration [96, 118-120]. Thereby, the applied magnetic field, system efficiency and accuracy are controlled.

In this study, it is aimed to present a density-based quantitative method for detection of adipogenic differentiated bone marrow cells using magnetic levitation system. Hypothesis of the study bases on density changing as a consequence of accumulated low-density lipid droplets during adipogenic induction. Due to lower density of adipocytes when compared to stem cells or other cell types, it seems possible to detect adipocytes in a heterogeneous population. This system could be a preferable candidate to detection techniques with its cost-effective, label-free principle and operational simplicity.

CHAPTER 2

MATERIALS AND METHODS

2.1. Principle of Magnetic Levitation System and Experimental Setup

In the paramagnetic medium, cells tend to move towards lower magnetic field region when applying a magnetic field. The dominant forces on magnetic levitation are magnetic force (F_{mag}, Eq. 1), gravitational force and buoyancy force. When buoyancy force and gravitation force are evaluated as resultant forces, it is called as corrected gravitational force (F_g, Eq. 2). In the levitation system, the applied magnetic force, where V is cell volume, $\Delta\chi$ is magnetic susceptibility difference between particle/cell and paramagnetic liquid, μ_0 is permeability of free space, B is magnetic induction and ∇ is the del operator, on diamagnetic objects are balanced with corrected gravitational force (Eq. 3), where $\Delta\rho$ is the density difference between cell and paramagnetic liquid, g is gravitational acceleration.

$$F_{mag} = \frac{V.\Delta\chi}{\mu_0}(B.\nabla)B \quad (1)$$

$$F_g = V.\Delta\rho.g \quad (2)$$

In the equilibrium position, the following equation is obtained;

$$F_{mag} + F_g = 0 \quad (3)$$

$$\frac{V.(\chi_{cell}-\chi_{medium})}{\mu_0}(B.\nabla)B = V(\rho_{cell} - \rho_{medium})g \quad (4)$$

According to equilibrium equation (Eq. 4), volume of the particles/cells is neglected during levitation. In the system, density and magnetic susceptibility play an active role. By increasing magnetic susceptibility of the paramagnetic liquid, F_{mag} is

increased and the cells are positioned at the point where the F_{mag} and F_g are balanced depending on their density.

In order to use this principle, magnetic levitation device was constructed with micro-capillary channel (1-mm × 1-mm cross-section, 50-mm length, and 0.2-mm wall thickness, Vitrocom) between two N52-grade neodymium magnets (NdFeB) (50-mm length, 5-mm height and 2-mm width, Supermagnete) and two mirrors (12.7× 12.7×3.2 mm, Thorlabs) placed at 45° to visualize levitation of cells using an inverted microscope (Olympus IX-83). Parts of levitation device were held with photoreactive resin (Clear v2 FLGPCL02) printed by 3D printer (Formlabs Form 2).

2.2. Cell Culture

D1 ORL UVA (mouse bone marrow stem cells) [121] and 7F2 (mouse osteoblasts) (ATCC) [95] were cultured in growth medium supplemented with 10% fetal bovine serum (FBS, Biological Industries) and 1% penicillin/streptomycin (Invitrogen) at 37°C in a 5% CO_2 humidified incubator. D1 ORL UVA was cultured in Dulbecco's Modified Eagle's medium (DMEM high glucose, Gibco) whereas 7F2 cells in alpha minimum essential medium (αMEM, Sigma) with 2 mM L-glutamine and 1 mM sodium pyruvate. The growth medium was refreshed every 2-3 days and the cells were passaged by using 0.25% trypsin/EDTA solution (Biological Industries) during 5 minutes when they reached approximately 80-90% confluence (every 4-6 days). The cells were used in studies until passage 40.

2.3. Adipogenic Differentiation

For adipogenic differentiation of D1 ORL UVA cells, the cells were seeded into 24-well plates with the concentration of 1000 cells/well. After 2 days, the growth medium (DMEM) was replaced with the induction medium containing 10 nM dexamethasone (Sigma), 50 mM indomethacin (Sigma), $5x10^{-3}$ mg/ml insulin (Sigma) and the cells were cultured during 15 days by refreshing every 2-3 days. Similarly, 7F2 cells were induced over 10 days in αMEM supplemented with inducing agents in 6-well plates with the

concentration of 5000 cells/mL. Images of both cell types were taken at 10X using an inverted microscope (Olympus IX-83). Differentiated cells were stained with Oil-red- O to visualize lipid accumulated cells at 10^{th} day of induction. For staining, cells were washed with 1X PBS twice and stained for 45 min at 37 °C with 60% diluted Oil-red- O in PBS. Then, the cells were rinsed (x3) with PBS. Lipid droplets were monitored by the inverted microscope.

2.4. Magnetic Levitation of Polymer Beads

In order to determine density gradient in magnetic levitation device, polymeric beads with three different densities; 1 g/mL, 1.02 g/mL (size: 10-20 μm) and 1.09 g/mL (size: 20-27 μm) (Cospheric LLC., ABD), were used. They were levitated in the culture medium including 25 mM, 50 mM or 100 mM gadolinium (Gd^{3+}) (Gadavist®, Bayer) and the levitated beads in all concentrations were monitored under the inverted microscope at 4X. Images of beads in the magnetic levitation platform were taken after reaching equilibrium position about 10 minutes. The levitation heights of the beads which were determined as distance from the upper limit of the bottom magnet were calculated by using Image J Fiji software.

2.5. Magnetic Levitation of the Cells

D1 ORL UVA cells cultured in growth and adipogenic induction medium were trypsinized with 0.25% trypsin/EDTA solution at 1^{st}, 5^{th} 8^{th},12^{nd} and 15^{th} days, and the cell suspension was centrifuged (Eppendorf) at 125 × g for 5 min. Pellet was resuspended to 10^5 cells/mL in the culture medium and each sample with 50 μl per capillary (5000 cells/capillary) were loaded into the microcapillary after adding Gd^{3+} paramagnetic agent with concentrations of 25 mM, 50 mM and 100 mM. When the cells reached the equilibrium position within 10 min, the levitated cells were imaged under an inverted microscope. Then, the analysis of levitation images of the cells was done by Image J Fiji software to determine levitation heights, density and cell size. Likewise, 7F2 cells were

trypsinized at 1st, 5th and 10th days and levitated in the medium containing 25 mM Gd^{3+} concentration and levitation images were analyzed using same analysis method.

2.6. Cell Viability Assay

D1 ORL UVA cells were seeded at a concentration of 1×10^3 cells/well in a 24-well plate and cultured for 22 days. Cell viability was tested by staining kit (calcein-AM/propidium iodide, Sigma Aldrich) for fluorescence staining of viable and dead cells after 22 days to check viability of levitated cells. For that, calcein-AM and propidium iodide solutions were added into PBS with the concentration of 2 μm/mL and 1 μm/mL, respectively. The cells were washed with PBS. After trypsinization of cell, cells were suspended in PBS and 100 μm assay solution was added into the cell suspension ($1x10^5$ cells/mL) and incubated at 37 °C for 15 min. Then, the cells were levitated using three different concentrations of Gd^{3+} (25, 50 and 100 mM). Levitated cells were monitored under the fluorescence microscope (Olympus IX-83) for simultaneous imaging of live (green-excitation: 490 nm, emission: 515 nm) and dead (red-excitation: 535 nm, emission: 617 nm) cells.

2.7. Fluorescent Staining and Mixing of D1 ORL UVA and 7F2 Cells with Different Ratios

D1 ORL UVA cells cultured in growth medium (DMEM) were trypsinized and the cells obtained by centrifugation were resuspended at a density of 1×10^6 cells/mL in serum-free DMEM. Then, DiO (green) cell-labeling solution (VybrantTM) was added with the concentration of 5 μM and incubated at 37°C in the incubator for 20 min. After incubation, the labelled cell suspensions were centrifuged at 1500 rpm for 5 min and the supernatant was removed. Pellet was resuspended in medium. The wash procedure was repeated two more times. The same protocol was applied for 7F2 cells cultured in αMEM growth medium and adipogenic induction medium. The cells were trypsinized and then resuspended at 10^6 cells/mL concentration in serum-free medium. Later on, the cells were stained with 5 μM of DiI (red) cell-labeling solution with the same protocol. After staining

step, labelled D1 and 7F2 cells were mixed at different percentages of 7F2 cells with 50%, 25%, 10%, 5% and 1% in medium containing 25 mM Gd^{3+} and levitated in magnetic levitation device. The cells were monitored using the fluorescence microscope (Olympus IX-83).

2.8. Statistical Analysis

During the study, all experiments were repeated in triplicate. Density and levitation height data were presented with the mean and standard deviation (mean ± SD). To determine statistical difference, Student's t-test (two-tail) or one-way ANOVA with Tukey's multiple comparisons test were used and $P < 0.05$ was considered as statistically significant. The associations between observed and expected cell ratios in levitation device were tested by using Chi-square test. Graphs showing levitation height versus density of beads at different Gd^{3+} concentrations were plotted and linear regression over the data was performed to obtain equations providing density of levitated particles/cells levitated in the magnetic detection system.

CHAPTER 3

RESULTS AND DISCUSSION

3.1. Calibration of the Magnetic Levitation System with Polymeric Beads

In this study, it was used magnetic levitation platform composed of two neodymium magnets with same poles facing each other to create magnetic force, a capillary channel to load cells in a paramagnetic medium, and two parallel mirrors to visualize levitated cells in real time (Figure 5A). By generating magnetic force with permanent magnets, the corrected gravitational force (F_g) which is the combination of gravitational force and buoyancy force (F_b) on cells was balanced (Figure 5B). By FEM simulation magnetic field gradient in used system and measurable cell density range was determined for different Gadavist concentrations (Figure 5C-D). Results of simulation showed 10 mM Gd^{3+} indicated the best resolution value at 0.0000591 (g/mL) per micrometer distance (Figure 5E), however, the study was performed using Gd^{3+} concentration over 25 mM due to limited range of densities at 10 mM.

In previous studies, this system was used for the detection and characterization of cancer cells in blood cell populations and drug testing on prokaryotic cells [122]. Also, it was reported it could be used as a handheld platform for point-of-care testing for some diseases such as anemia and sickle cell disease since these diseases are characterized by density changing [123-126]. Here, we aimed to adapt the reported system to adipogenic cell detection by density-based separation principle.

To calibrate the microfluidic device for density-based detection of adipogenesis, polymeric beads with three different densities (1 g/mL, 1.02 g/mL and 1.09 g/mL) were levitated in the medium with paramagnetic agent Gadavist (Gd^{3+}) at 25, 50 and 100 mM concentrations and levitation profile of the beads was determined (Figure 6A). When the density of the beads decreased, the levitation heights of beads, which is described as distance from the upper surface of the bottom magnet, increased for all Gd^{3+} concentrations. Similarly, polymeric beads were positioning at higher levels when the

concentration of Gd^{3+} increased and it was observed that the distance between levitated beads with different densities was decreased with increased Gd^{3+} concentration in the medium. When the beads with 1.09 g/mL and 1 g/mL were levitated in the paramagnetic medium containing 25 mM Gd^{3+} concentration, the difference between the beads was found to be 425 µm and it was decreased to 261 µm and 156 µm for 50 mM and 100 mM Gd^{3+}, respectively (Figure 6, blue arrows). Namely, the height of beads with the density of 1 g/mL was 59.11%, 29.64% and 15.96% higher than the beads with 1.09 g/mL density in the medium including 25 mM, 50 mM and 100 mM Gd^{3+} concentration, respectively (all $p<0.05$). Similarly, the differences between the levitation heights of beads with densities of 1.09 g/mL and 1.02 g/mL were 346 µm, 203µm and 116 µm for 25 mM, 50 mM and 100 mM concentrations of Gd^{3+}, respectively (Figure 6, red arrows). Furthermore, the levitation height of beads with 1 g/mL and 1.02 g/mL density was very c lose, which difference is 40 µm at 100 mM, 58 µm at 50 mM and 79 µm at 25 mM Gd^{3+} concentrations. Namely, results showed that the ability to distinguish the system was reducing with increased paramagnetic agent concentration.

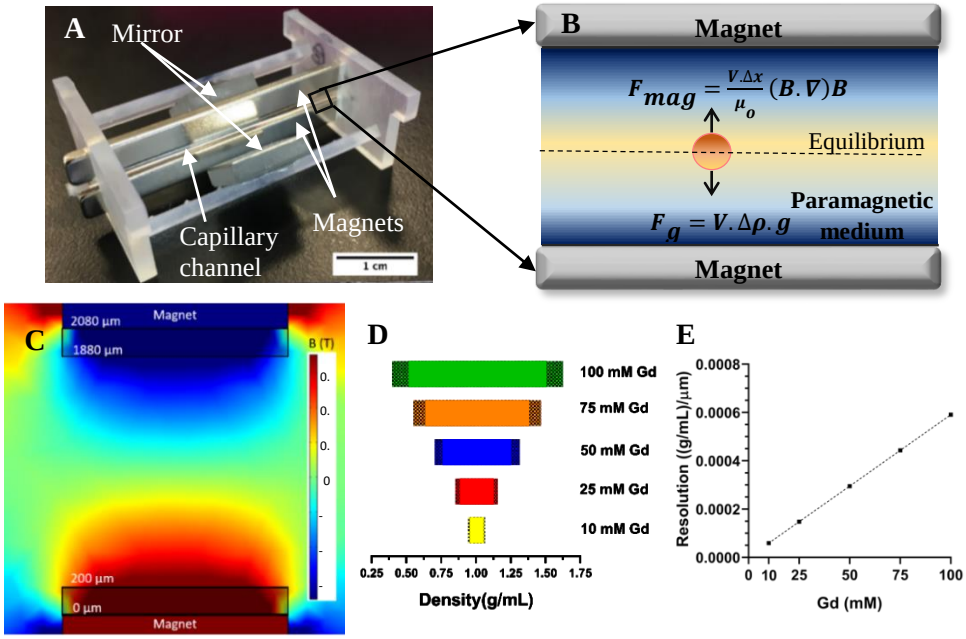

Figure 5. Magnetic levitation device and its working principle. (A) Magnets, capillary channel and mirrors placed at 45˚ were used to contruct levitation device. (B) Representative image of magnetic and corrected gravitational forces which impact cell equilibrium position in levitation device. (C) Cross-sectional representation of the magnetic induction between permanent magnets. (D) Density range that can be measured with respect to used Gd^{3+} concentrations. (E) Resolution of the levitation system with respect to used Gd^{3+}.

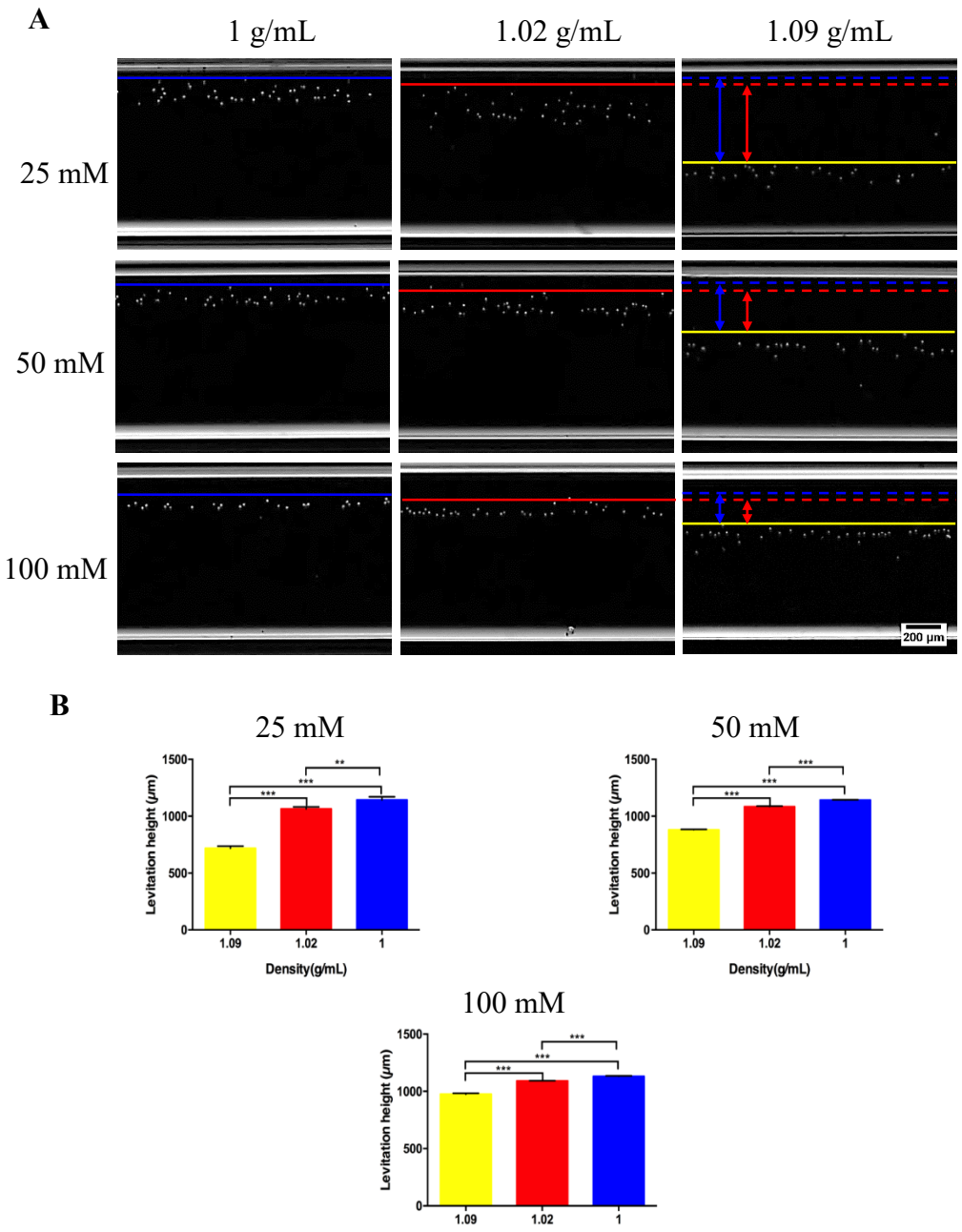

Figure 6. Calibration of the levitation system by using density-known polymeric beads. (A) Micrographs of levitation of polymeric beads with densities of 1 g/mL, 1.02 g/mL and 1.09 g/mL in medium containing 25, 50 and 100 mM Gadavist. Solid lines show maximum point of levitated beads and red and blue arrows present difference of density of 1.09 g/mL with 1g/mL and 1.02 g/mL, respectively. Scale bar: 200 µm. (B) Levitation heights of the polymeric beads in medium containing 25 mM, 50 mM and 100 mM Gd^{3+}. Data are presented as mean of replicates with error bars (±SD). One-way ANOVA with Tukey's multiple comparisons test was performed for statistical. analysis. Statistical significance was defined as *: $p<0.05$; **: $p<0.01$; ***: $p<0.001$.

According to average density and levitation height values, it was demonstrated that there was inverse relationship between density and levitation height, and linear equations were obtained for three different Gd^{3+} concentrations (Figure 7). Linear equations allowing to calculate density by using levitation heights of single cells showed strong correlation with $\rho = - 0.000209001 * h + 1.240573$ ($R^2 = 0.998$); $\rho = -0.000344456 * h + 1.393534$ ($R^2 = 0.999$), $\rho = -0.000583928 * h + 1.659352$ ($R^2 = 0.998$), where ρ corresponds to the density (g/mL) and h corresponds to the levitation height (μm) for 25 mM, 50mM and 100 mM, respectively.

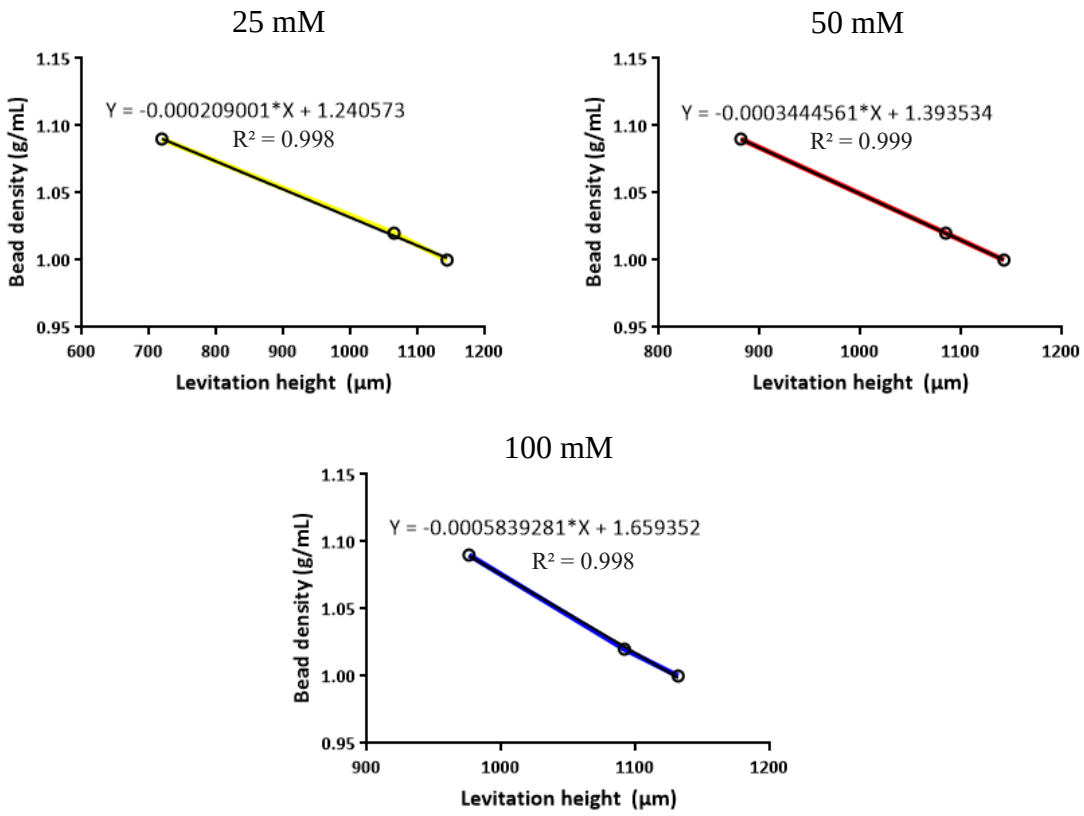

Figure 7. Linear fits obtained from average heights of beads for three Gadavist concentrations (25 mM, 50 mM and 100 mM).

3.2. Detection of the Adipogenic Cells with the Microfluidic Platform

Initially, bone marrow stem cells (D1 ORL UVA) were used as an experimental model in the study and they were cultured in adipogenic medium up to 15 days in parallel with culture in growth medium as a control group (Figure 8). Lipid accumulation

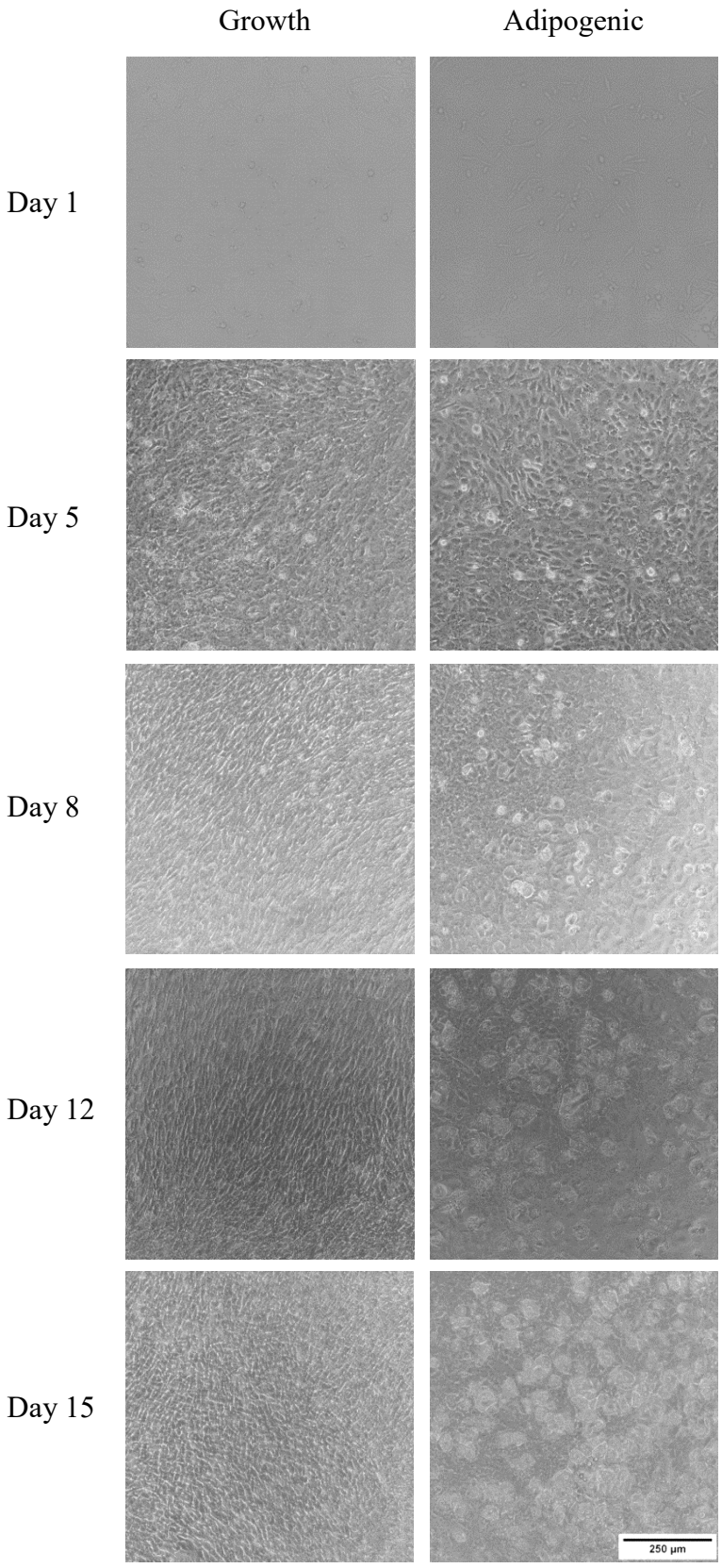

Figure 8. Culture images of D1 ORL UVA cells cultured in growth and adipogenic medium during 15 days. Scale bar: 250 µm

in cells started at the end of the first week of the culture. After 15 days of culture in adipogenic and growth media, the cells were levitated in magnetic levitation device with Gadavist concentrations of 25 mM, 50 mM and 100 mM (Figure 9). One of the reasons for using this concentration range and paramagnetic agent was to avoid the cytotoxic effect of Gd^{3+}, which is a lanthanide metal [93]. Gd^{3+} (107.8 pm) has a similar size to Ca^{2+} (114 pm) which has an important role on biological processes and this similarity may cause competitive inhibition and toxic effect during the processes [93, 127]. Cytotoxicity of Gd^{3+} can be prevented with chelate forms of Gd^{3+}. Considering previous studies determining the effect of different chelating forms on cell proliferation and toxic range of Gd^{3+}, in this study, it was used nontoxic concentration range (≤100 mM) and nonionic, macrocyclic chelate form (Gadobutrol, Gadavist®) of Gd^{3+} [109, 128].

Consistent with the results obtained by the levitation of polymeric beads, the distance between adipogenic cells with lower density and bulk population of denser cells increased when lower Gd^{3+} concentrations were used. When the cells were levitated in medium containing 100 mM Gd^{3+}, the distance between the average levitation height of the population and the lipid accumulated cells located at the highest level was 225 µm. However, it increased to 273 µm (21% increasing) and 377 µm (67% increasing) as the concentration of Gd^{3+} was reduced to 50 mM and 25 mM, respectively (Figure 9). As a result of the increased sensitivity of levitation system to density changes of cells by using decreased Gd^{3+} concentration, 25 mM Gd^{3+} concentration was found appropriate to use for density-based detection of the adipogenic cells in the magnetic levitation system and the further experiments were carried out using this concentration.

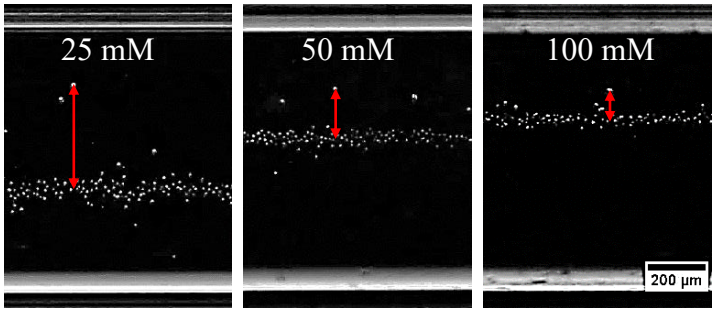

Figure 9. Optimization of the paramagnetic medium concentration for adipocyte detection. Red arrows indicate difference between levitated bulk cell population and differentiated cells with highest levitation level. Scale bar: 200 µm

At previous studies based on magnetic levitation, it has been shown that the dead cells tended to collapse to the bottom surface of the capillary due to increased cell density [122]. To reveal levitated cells including also lipid-accumulated cells were only healthy cells when levitated with 25 mM Gd^{3+}, an in situ live/dead staining was performed. Almost all cells located at the analysis region were alive (Figure 10, green cells).

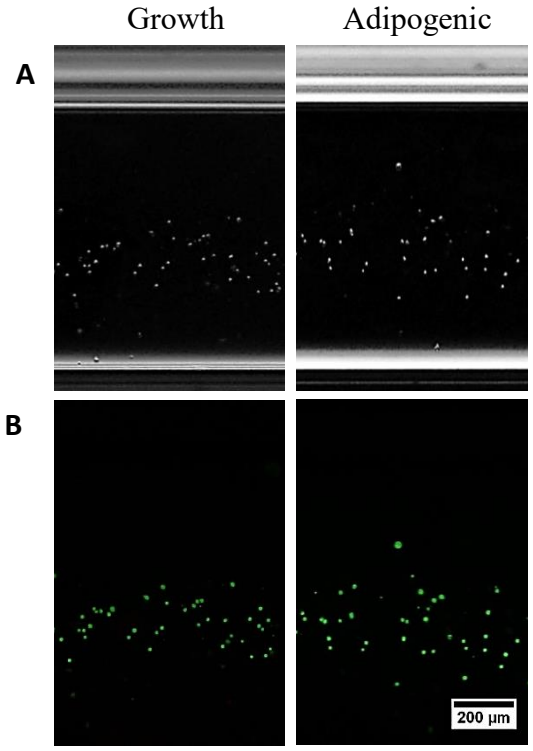

Figure 10. Live/dead staining of levitated D1 ORL UVA cells at 22nd day of culture. The cells cultured in growth and adipogenic medium were stained with calcein/PI and levitated using 25 mM Gd^{3+} (Green:alive cells and red:dead cells). Scale bar: 200 µm.

3.3. Determination of Density Profiles of Adipogenic Cells

The effect of adipogenesis on levitation height of the cells in capillary channel was examined with D1 ORL UVA cells cultured in culture plates over 15 days. The cells were levitated at certain intervals (day 1, 5, 8, 12 and 15) by using determined Gadavist concentration (25 mM Gd^{3+}) and they reached the equilibrium position in levitation system in about 10 minutes. The short process time and high throughput in the system

was one of the reasons why this method was a preferable alternative to other detection techniques [57, 70]. For instance, SMR system offers measuring of cell density with 500 cells/hour [57]. On the contrary, to measure density with relatively high throughput (approximately 5000 cells in one case) is possible by using levitation device. After cells rapidly reached to equilibrium position in capillary, the obtained levitation images were analyzed to control changes in density of the induced cells. It was observed that levitation heights were similar for both growth and adipogenic cells at the first day of culture, whereas a little part of cell population associated with adipogenic induction were located at higher levitation levels at 15th day (Figure 11). Results showed that the cells in growth medium were positioned at 761 ± 49 μm from bottom magnet and, the average density of the cells were measured as 1.081 ± 0.010 g/mL at first day by using previously obtained equation describing the relationship between levitation height and density values for 25 mM Gd^{3+}. The lowest density of growth cells was 1.059 g/mL corresponding to levitation height of 869 μm. After adipogenic induction, cells still had similar average density with 1.080 ± 0.008 g/mL (768 ± 37 μm of levitation height) and 1.078 ± 0.010 g/mL (777 ± 49 μm) for growth and adipogenic cells, respectively, at 5th day of culture. At day 15, the lowest density (1.052 g/mL ~ 903 μm) of the cells observed in the undifferentiated cell population was similar to that of the first day. However, with following days of induction, the observed lowest density decreased to 1.023 g/mL (~1042 μm of levitation height), 1.024 g/mL (~1035 μm) and 1.007 g/mL (~1115 μm) in adipogenic induced cells at 8th, 12nd and 15th days of culture, respectively. Namely, adipocytes were positioned at higher levels due to accumulation of lipid droplets primarily formed by triacylglycerols with a density below 1 g/mL [129, 130]. However, during adipogenic differentiation, the cells were located dispersed positions at higher levels after adipogenic induction. This heterogeneity may result from changing lipid droplet amount and morphology in response to the inducing agents and cell to cell interactions [131-133]. During experiments, the average density of adipogenic group did not change significantly ($p>0.1$ for all days except day 8) although the decrease in density of adipogenic induced cells. Because numbers of lipid-accumulated cells located at higher levitation levels was not enough to change average density values. Therefore, to enhance our understanding of individual differences between cell densities of two cell groups, skewness of cell density distribution and the lowest 5th percentile of population was evaluated (Figure 12). The average densities of cells in the lowest 5th percentile for cells cultured in growth and adipogenic medium were similar with values of 1.071 ± 0.008 g/mL and 1.073 ± 0.003 g/mL, respectively ($p=0.71$)

at first day. Also, the cells showed positive skewed distribution in both groups. Skewness of cell density distribution was similar between control and adipogenic cells with 1.9 ± 0.5 and 1.9 ± 0.3, respectively (p=0.94). At day 5, difference between average densities of the cells in the lowest 5th percentile in growth and adipogenic induction medium (p=0.98) and skewness values for these cell groups (p= 0.99) were still similar. After 8 days, average densities in 5th percentile for the cells started to be lower than that of the control group (p<0.01). At 8th day, average density of the cells residing in the lowest 5th percentile was 0.8% lower in adipogenic-induced group with average density of 1.058 g/mL (p<0.01) compared to controls with 1.067 g/mL, and 0.67% of the adipogenic population had smaller density values compared to the lowest density recorded on control cells (1.055 g/mL) at day 8. Skewness of the cells for growth and adipogenic cells was 1.0 ± 0.4 and -0.2 ± 0.6 (p=0.15). The lowest 5th percentile of adipogenic cell density was %1.2 (p=0.03) and %1.8 (p=0.03) lower than control cells at day 12 and 15, respectively.

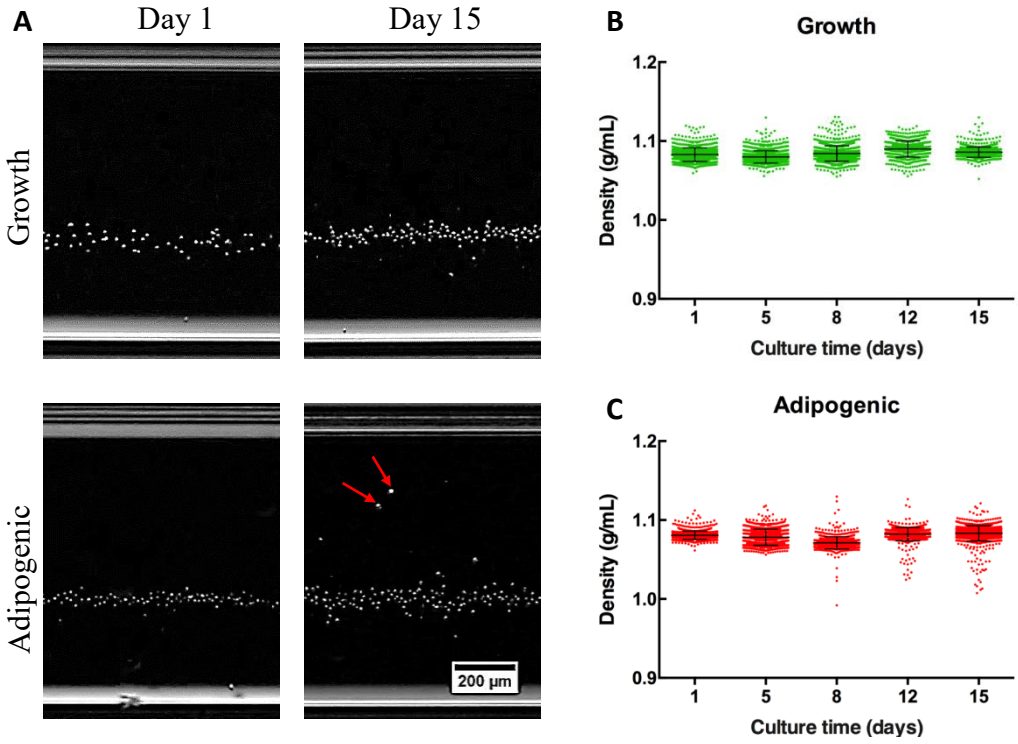

Figure 11. Levitation and density profiles of D1 ORL UVA cells levitated with 25 mM Gd^{3+}. (A) Undifferentiated and adipogenic-differentiated D1 ORL UVA cells were levitated at day 1 and 15. Red arrows show differentiated cells with lower densities. Scale bar: 200 µm. (B, C) Scatter plots of densities of growth and adipogenic cells at day 1, 5, 8, 12 and 15. Data are represented as scattered with an inset of mean ± SD.

Also, 1.8% of the adipogenic population had smaller density values than the lowest density of growth cell group (1.052 g/mL) at day 15. Furthermore, skewness for cells cultured in growth and adipogenic medium was 0.99 ± 0.6 and -2.3 ± 0.6 (p=0.02), respectively. As a result, negative skewness of density was increased due to the positioning of lipid-accumulated cells at higher levels and density of the cells at 5th percentile decreased as time progressed. Also, when the density distribution of population at certain days was analyzed, it was seen a changed pattern at low-density distribution of adipogenic group at day 12 and 15, especially (Figure 13). There were no any cells with a density below 1.05 g/mL up to 8th day, however, percentage of low-density cells was gradually increased up to 15th day. For all days except day 8, the cells were around 1.08 g/mL density for undifferentiated stem cells and it was consistent with previously determined densities of bone marrow-derived cells [134]. Although there is limited information about adipose density in the literature, the density range of adipose tissue was recorded as 0.92-0.97 g/mL [135, 136]. In the study, it was seen that density of the cells after adipogenic induction reduced to ~1.01 g/mL.

Increased cell size is associated with metabolic functions including secretion of cytokines and metabolism rate of adipocytes, and is one of the main characteristics during adipogenesis [4, 68, 137]. In previous studies, it has been shown that there was a relation between size changing of adipocytes and obesity and obesity-related diseases [138]. Therefore, determination of adipocyte size is one parameter for cellular studies on adipocytes and related diseases. Here, the size of levitated cells was measured from levitation images by software.

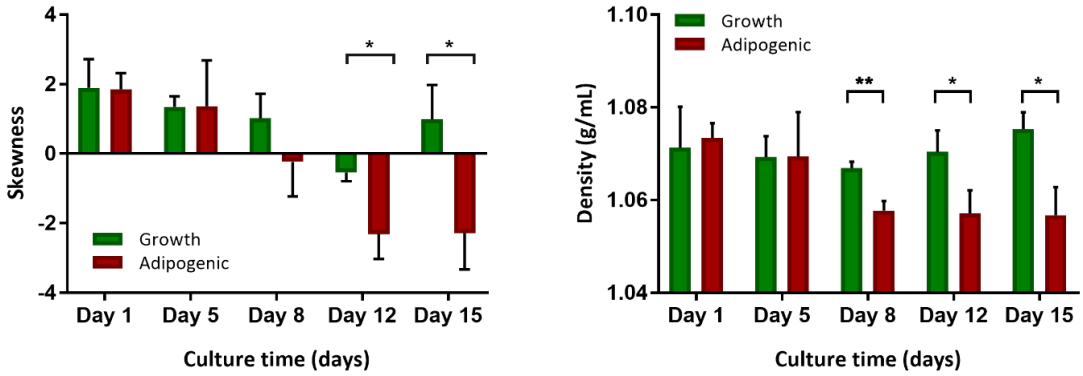

Figure 12. Skewness and lowest 5th percentile of densities of growth and adipogenic cells up to 15 days. Data are represented as mean ± SD. *: p<0.05; **: p<0.01; ***: p<0.001.

In analysis, the cells with density below the average density of growth cells (<1.084 g/mL) in all days were taken into consideration to measure cell size (Figure 14). At the first day, the average cell size of growth and adipogenic cells was 51±18 μm^2 and 36±19 μm^2, respectively, and the significant difference was not observed between them (p=0.06). After adipogenic induction, size of adipogenic cells increased to 45±28 μm^2 in average at day 15 (p=0.05) (Figure 14A). The number of cells with larger size than the average of growth cell size increased from 12% to 17% in population during adipogenesis. As presented previously, adipocytes show wide range of size depending on accumulated lipid droplets [15, 27]. During the study, it was seen different amount of lipid accumulation and also, the correlation between size and density was observed, rather than being a minor correlation (R^2=0.29) in contrast to undifferentiated cells (R^2=0.01) at day 15 (Figure 14B).

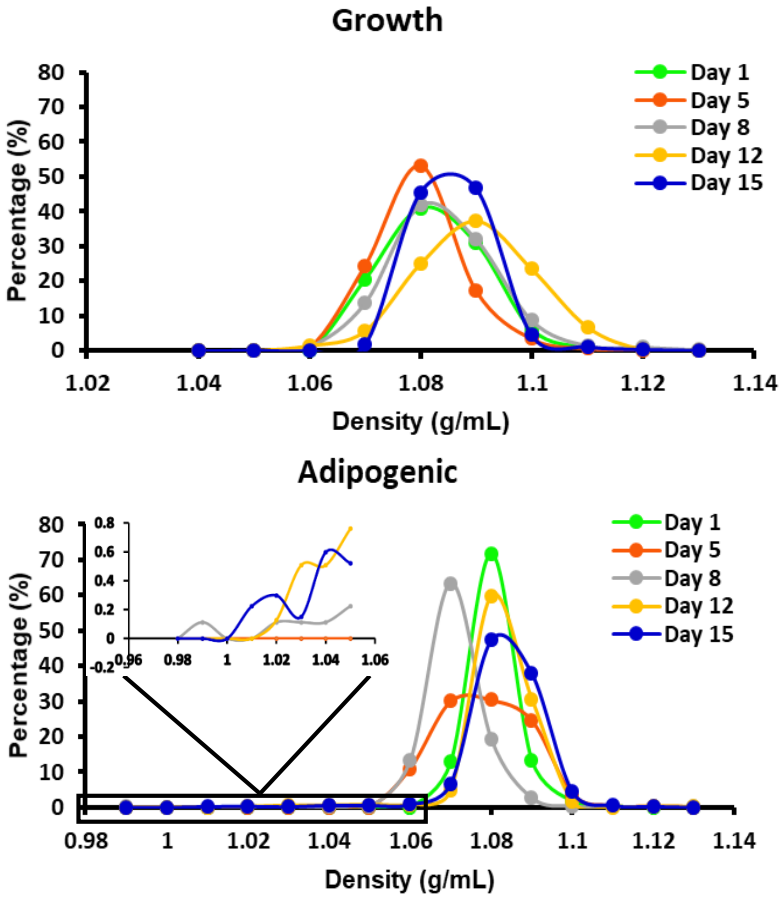

Figure 13. Density distribution of differentiated and undifferentiated D1 cells during 15 days.

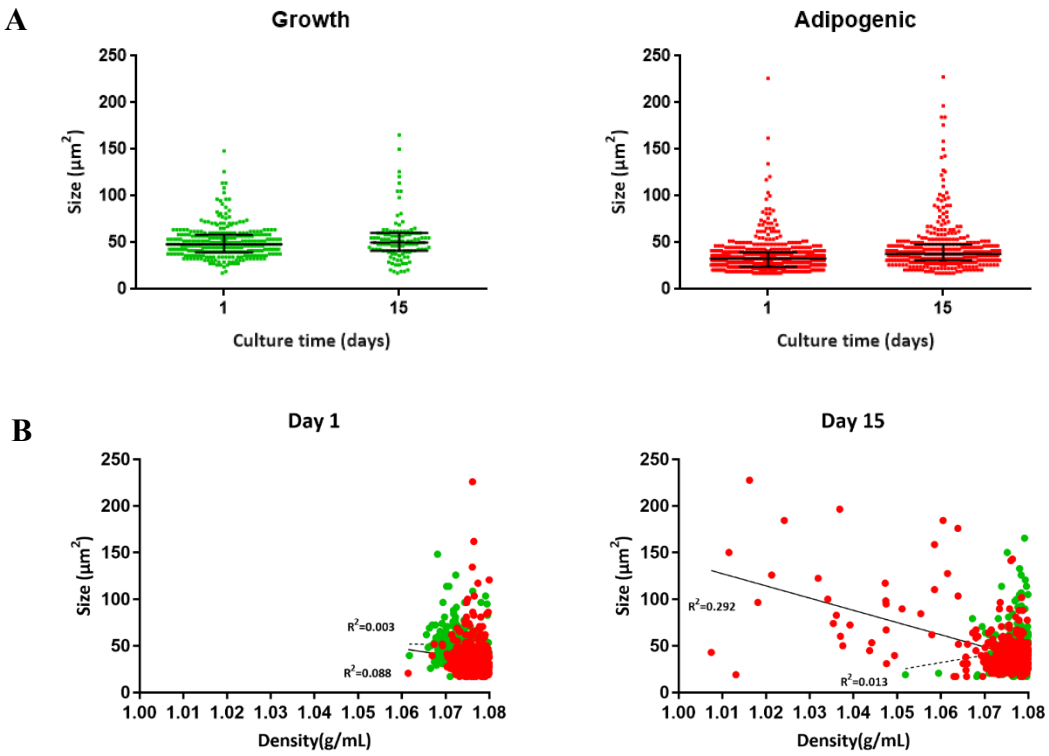

Figure 14. Cell size (area, µm^2) changing during adipogenic differentiation. (A) Scatter plot of size of growth and adipogenic-differentiated cells with density values below 1.084 g/mL (average density of the growth cells) at 1st and 15th days of culture. Data are represented as mean ± SD. (B) The relationship between cell size and density of adipogenic differentiated and undifferentiated D1 ORL UVA cells. Dashed and solid lines indicate linear regression for growth and adipogenic cells, respectively.

On the other hand, during culture of the cells, it was seen that long culture time might affect the cell density. When the cells were cultured over 22 days, cell density resulted in heterogeneous distribution of both growth and adipogenic groups (Figure 15), possibly, because of the fact that some factors (e.g. osmolarity and cell cycle) could affect cell density during long culture time [139-141]. Therefore, it was continued to the studies with 7F2 cells, which are bone marrow-derived cell line, with high amount accumulation ability of lipid droplets in relatively short time compared to D1 ORL UVA cells. The cells were cultured in growth and adipogenic medium for 10 days (Figure 16A) and they were stained with Oil-red-O at day 10 to show lipid accumulation during adipogenesis (Figure 16B). The cells were levitated with 25 mM Gd^{3+} at 1st, 5th and 10th days of culture (Figure 17A-B). The density of adipogenic cells was measured as 1.079±0.005 g/mL at day 1 and it decreased to 1.072±0.013 g/mL and 1.060±0.029 g/mL at day 5 and 10, respectively.

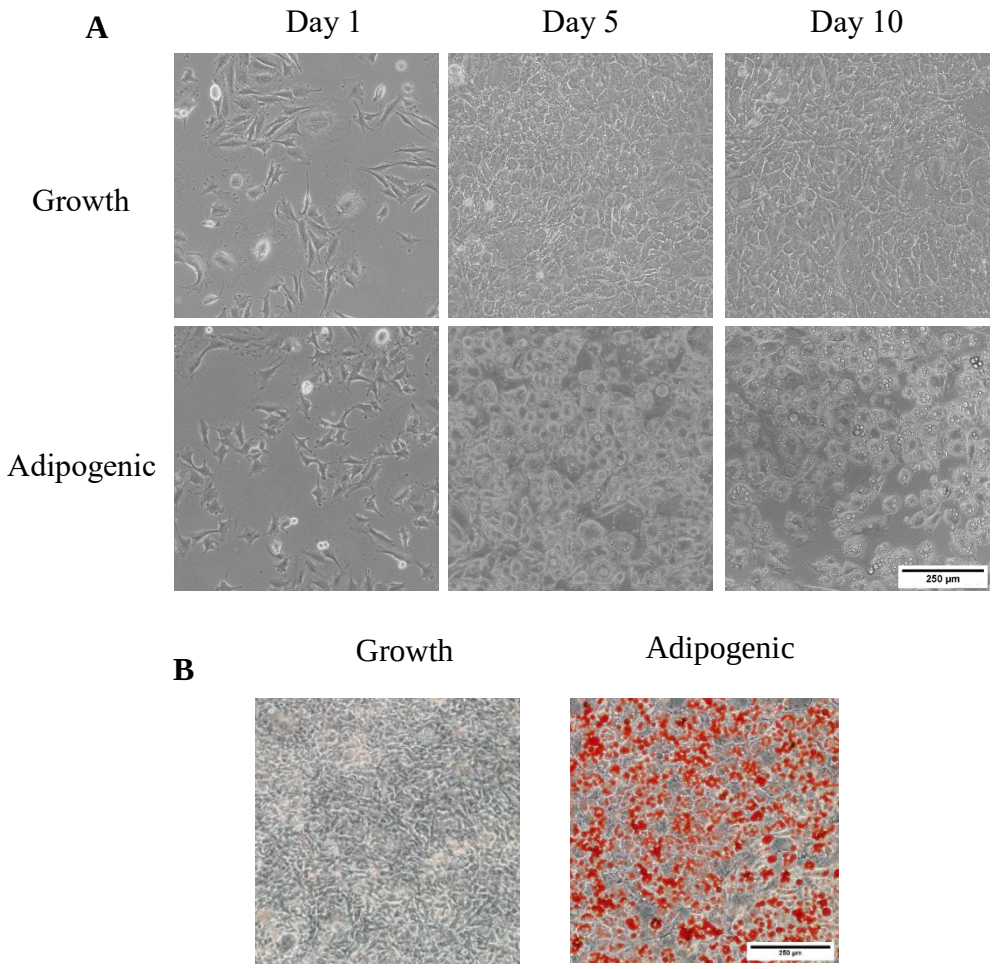

Figure 15. Culture images of 7F2 cells. (A) Culture images of the 7F2 cells in standard and adipogenic medium during 10 days. (B) Oil-red-O staining of 7F2 cells at 10th day of induction. Scale bar: 250 µm.

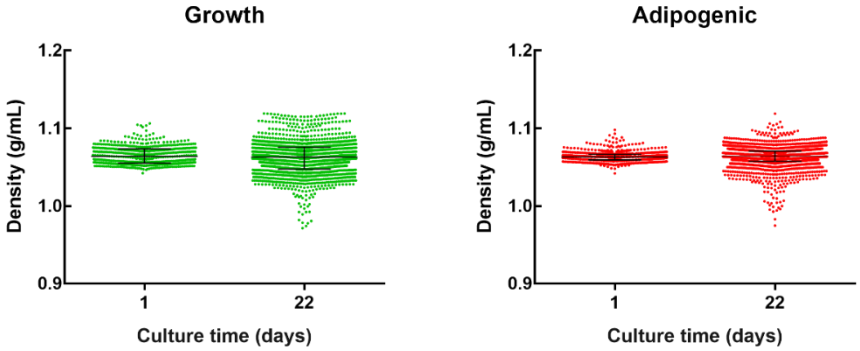

Figure 16. Scatter plot of growth and adipogenic-differentiated D1 ORL UVA cells at 1st and 22nd days of culture. The cells showed bilateral expanding at 22nd day.

Also, in 5th percentile for adipogenic-induced 7F2 cells, the average density decreased to 1.003 ± 0.004 g/mL including minimum density of 0.989 g/mL and 37% of the adipogenic cell population had lower density than the minimum density of growth cells (1.052 g/mL) at day 10. Furthermore, percentage of adipogenic cell population below average of the density of growth cells (1.071 ± 0.006 g/mL) consisted 61% (Figure 17C) and, the minimum density of adipogenic cells decreased 6.6% from day 1 to day 10 at 7F2 cells, whereas the density for adipogenic-differentiated D1 cells decreased 5.1% from day 1 to day 15. Thereby, it was demonstrated that the differentiation rate of 7F2 cells was more suitable for further studies due to providing high lipid accumulation within small time periods.

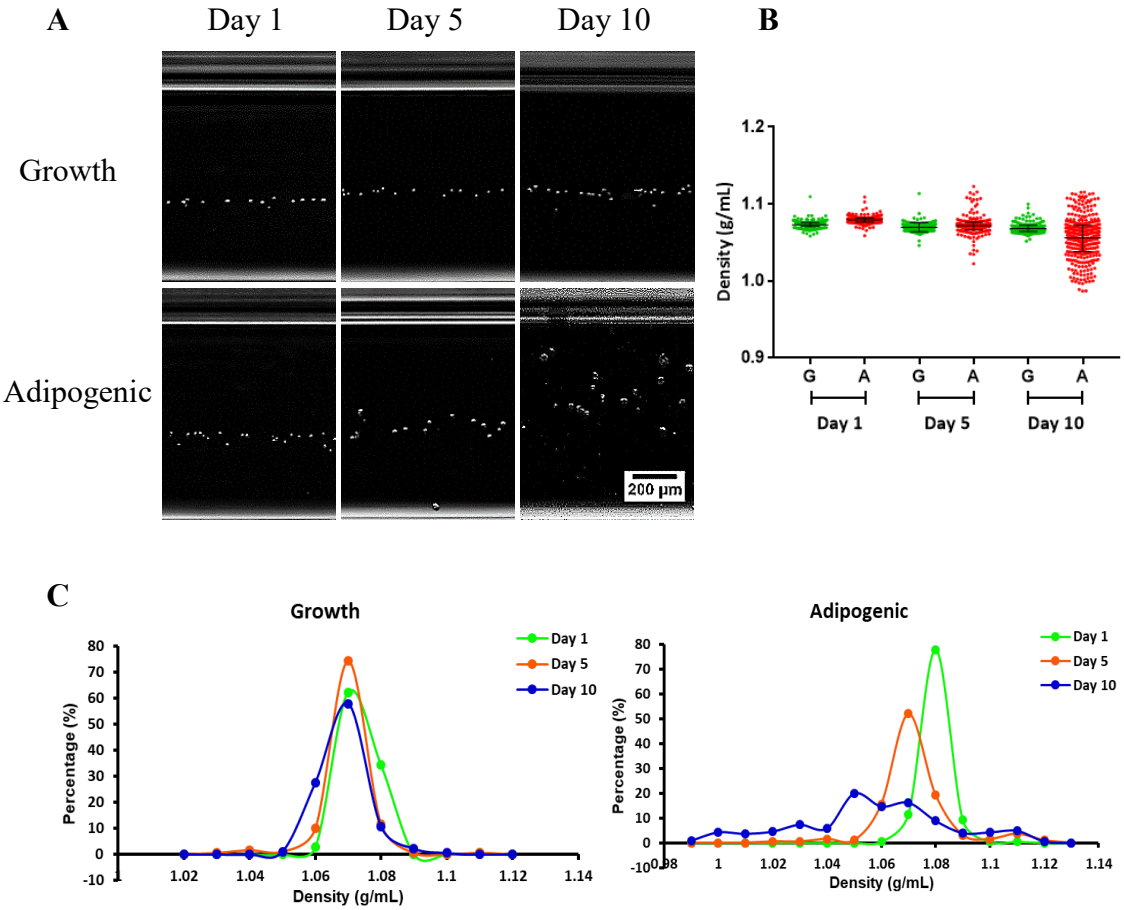

Figure 17. Levitation of 7F2 cells during 10 days. (A) Levitation micrographs of adipogenic differentiated and undifferentiated 7F2 cells during 10 days. (B) Scatter plot of densities of 7F2 cells. Data are represented as mean ± SD. (C) Density distribution of 7F2 cells.

3.4. Detection of Adipogenic Cells in Heterogeneous Cell Population with Stem Cells

To test adipogenic cell detection ability of the magnetic levitation system in a heterogeneous cell population, D1 ORL UVA cells (tracked green fluorescent dye) and 7F2 cells (tracked with red fluorescent dye) were mixed with different ratios and detected by using levitation system in medium containing 25 mM Gd^{3+}. To show that the differences observed in levitation height were based on differences in densities and not used cell type, it was levitated undifferentiated D1 ORL UVA and undifferentiated 7F2 cells with ratio of 50% at day 1, 5 and 10 as a control group (Figure 18) and it was shown the undifferentiated two cell types had similar density values ($p>0.05$) at all-time points. Also, undifferentiated D1 ORL UVA cells and adipogenic-differentiated 7F2 cells were mixed with different adipogenic 7F2 cell ratios; 1%, 5%, 10%, 25%, 50% (Figure 19).

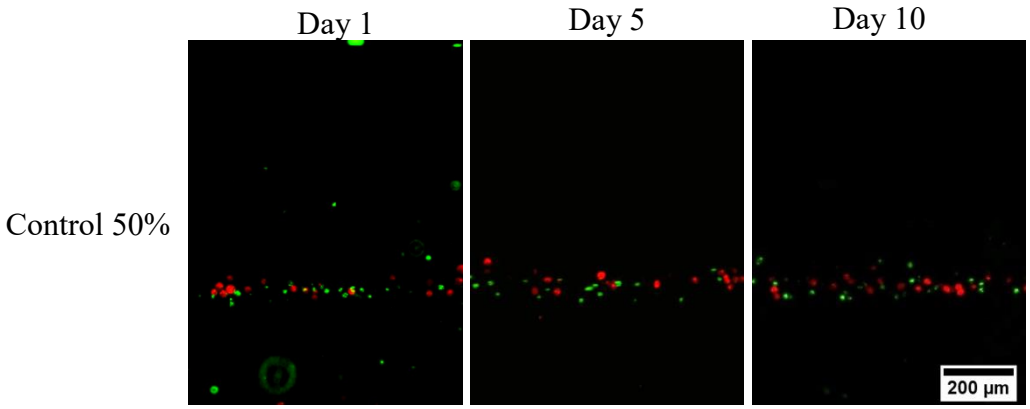

Figure 18. Fluorescence microscope images of the levitated heterogeneous population consisting of undifferentiated 7F2 (red) cells and D1 ORL UVA (green) cells mixed with 50% ratio. Scale bar: 200 µm.

After levitation of mixed two cell types, it was shown that the difference between the relative density of adipogenic-differentiated 7F2 cells and undifferentiated D1 ORL UVA cells increased with increasing culture period (Figure 20A). When undifferentiated stem cells and adipogenic cells were mixed at 50%, obtained average relative density was similar with 3.5% difference at the first day of culture ($p=0.45$), while there was 25.7%

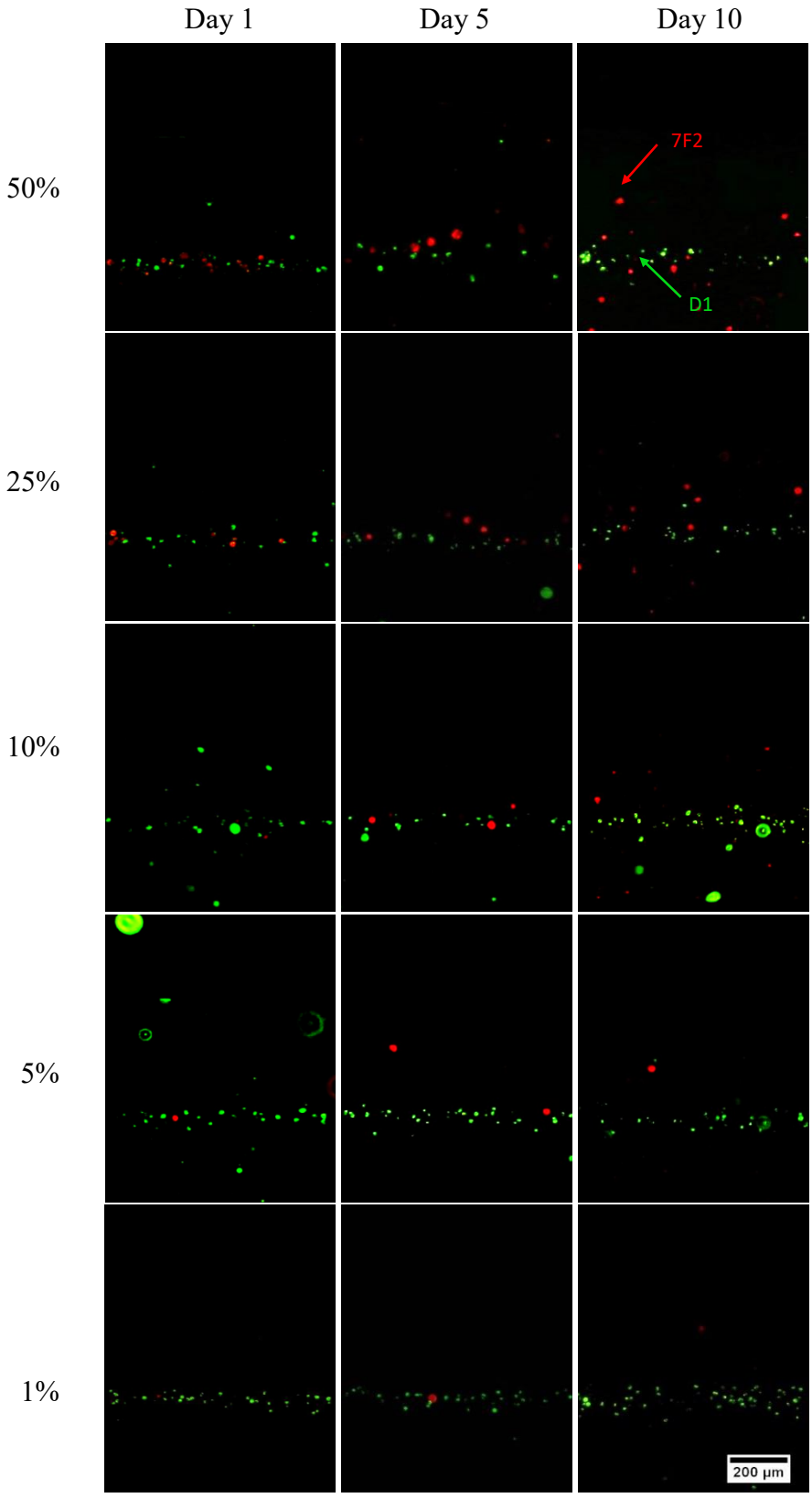

Figure 19. Fluorescent images of the levitated heterogeneous populations of undifferentiated D1 ORL UVA cells (green) and adipogenic differentiated 7F2 cells (red) with different ratios (50%, 25%, 10%, 5% and 1%) at 1st, 5th and 10th day. Scale bar: 200 µm.

($p<0.01$) difference between two cell groups at 10^{th} day of culture. Also, when it was compared the lowest 5^{th} percentile of adipogenic cells at day 1 with day 5 and 10, relative density difference increased 27.4% and 50.4%, respectively. It was observed similar trends for other ratios. Even if the proportion of adipogenic cells in the heterogeneous population was reduced to 1%, small amounts of low-density 7F2 cells were successfully detected in the levitation system.

Adipogenic cell fractions in the heterogeneous cell population were determined by manual counting of 7F2 and D1 cells. It was demonstrated that observed values were mostly similar ($p>0.05$) to expected values by chi-square test (Figure 20B). The statistical difference between observed and expected ratios at day 1 was possibly due to experimental mistake.

Finally, the cells were categorized with respect to levitation height and determined their lineages poststratification (Figure 21). Therefore, the capillary was divided into three density zones; zone I indicating the cells with density below 1.02 g/mL (Figure 21A, above yellow dashed line), zone II indicating the cells with density between 1.02 g/mL and 1.06 g/mL (Figure 21A, between blue and yellow dashed line lines), and zone III indicating the cells with density above 1.06 g/mL (Figure 21A, below blue line) and the distribution of two cell types at these three zones were determined (Figure 21B). In control group, 99%, 100% and 95% of D1 ORL UVA cells were located at zone III at day 1, 5 and 10 respectively. Similarly, 98% of 7F2 cells were located at zone III on all days and there were no any cells at zone I. Namely, two cell types occupied zone III with 50:50 ratio (Figure 21B). However, when the adipogenic-differentiated 7F2 cells and undifferentiated D1 ORL UVA cells were mixed with 50% ratio, percentage of 7F2 cells at zone III were decreased to 84% and 55% at 5^{th} and 10^{th} day. In parallel with this decreasing, 7F2 cells increased by 15% and 41% at zone II and, 1.5% and 4% at zone I at day 5 and 10, respectively. Namely, zone II consisted of 93% of adipogenic 7F2 cells and zone I was totally occupied by 7F2 cells in the following days of induction (Figure 21B). Even though the ratio of the 7F2 cells in heterogeneous population were decreased to 1%, at 10^{th} day of induction, it was detected 18% of the cells at zone I. Thereby, it was shown that the system was highly selective for lipid-accumulated cells in heterogeneous populations.

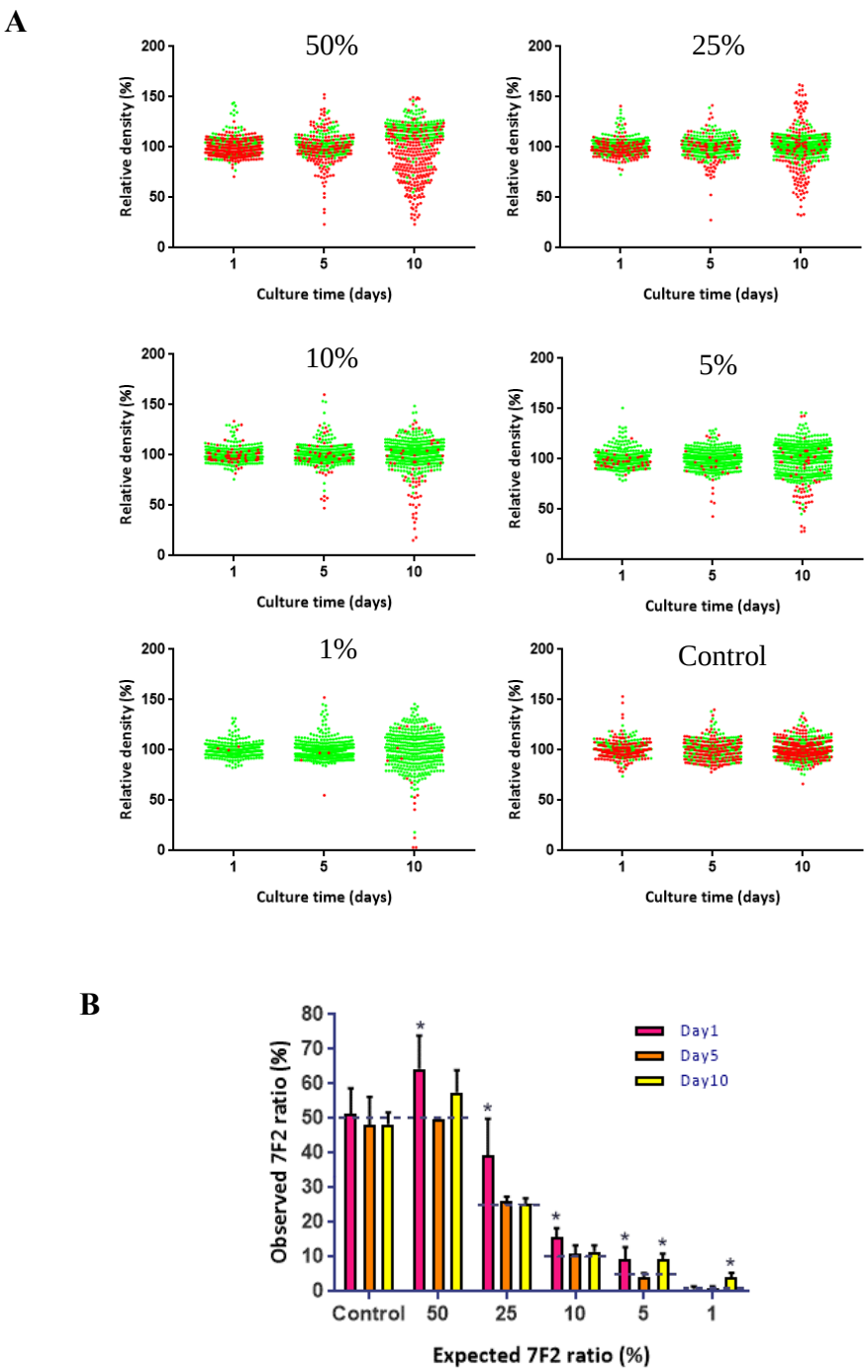

Figure 20. Detection of adipogenic cells in the heterogeneous cell population. (A) Scatter plot of the relative density (%) of adipogenic-differentiated 7F2 cells and undifferentiated D1 ORL UVA cells by mixing at different ratios of 7F2 cells (50%, 25%, 10%, 5% and 1%) and, mixing of undifferentiated D1 ORL UVA and 7F2 with 50% ratio as a control. (C) Observed ratios of 7F2 cells in the heterogeneous populations with the detection system using magnetic levitation. The chi-square test was performed for statistical analysis. Statistical significance was defined as *: $p<0.05$; **: $p<0.01$; ***: $p<0.001$.

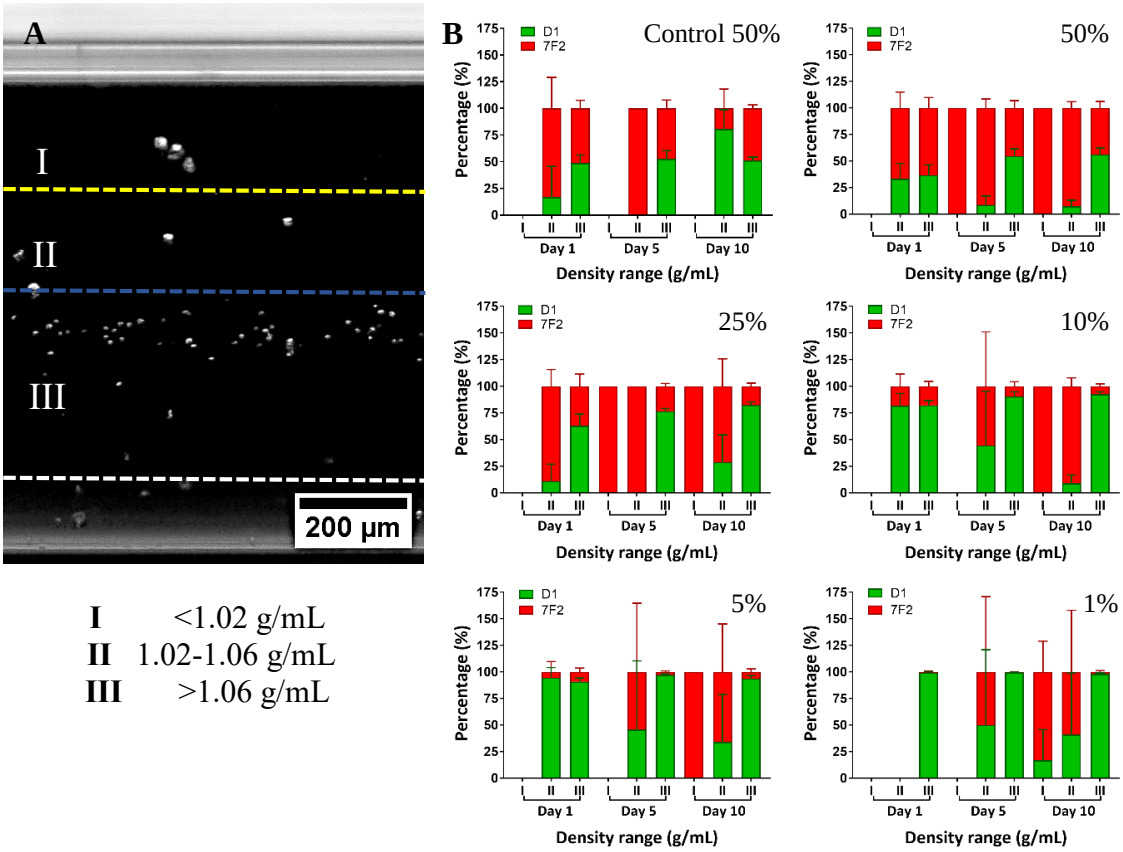

Figure 21. Categorization with regard to cell density with three zones (I: for <1.02 g/mL, II: for between 1.02 g/mL and 1.06 g/mL, III: for >1.06 g/mL and cell ratios in the zones.

CHAPTER 4

CONCLUSION

In this study, it was aimed to use magnetic levitation system for detection of adipogenic differentiation. D1 ORL UVA and 7F2 cells were used to obtain lipid-accumulated cells and they were individually levitated at certain intervals using appropriate paramagnetic agent concentration. Also, the detection of adipogenic cells in the heterogeneous population consisting of undifferentiated D1 cells and adipogenic differentiated 7F2 cells was performed by using the levitation system. In the study, the increase in the number of cells accumulating lipid droplets was clearly observed throughout culture of the cells. In addition, the size change in adipogenic-induced cells could be demonstrated by the method used. Accordingly, a correlation was observed between increasing the cell size in parallel with the decreasing of density in lipid-accumulated cells. As a result, it was demonstrated that increase in cell number and cell size that act as a marker of adipose tissue growth in obesity would be determined successfully using magnetic levitation system. Also, single-cell density measurement of adipocytes was performed first time by using levitation system. This system is a preferable alternative to other detection techniques with its performance with rapid and relatively high throughput, as well as cost-effective fabrication. This system, which is suitable for the detection of adipocytes, may enable to separate the adipocytes by modifications in system to obtain a continuous flow and to use it for detection of decreasing in the volume of lipid cells concomitant therapeutic studies.

REFERENCES

1. Mizuno, H.; Tobita, M.; Ogawa, R.; Orbay, H.; Fujimura, J.; Ono, S.; Kakudo, N.; Kusumoto, K.; Hyakusoku, H., Adipose-Derived Stem Cells in Regenerative Medicine. In *Principles of Gender-Specific Medicine*, Elsevier: 2017; pp 459-479.

2. Ali, A. T.; Hochfeld, W. E.; Myburgh, R.; Pepper, M. S., Adipocyte and adipogenesis. *European Journal of Cell Biology* **2013,** *92* (6-7), 229-36.

3. Rosen, E. D.; Spiegelman, B. M., What we talk about when we talk about fat. *Cell* **2014,** *156* (1-2), 20-44.

4. Skurk, T.; Alberti-Huber, C.; Herder, C.; Hauner, H., Relationship between adipocyte size and adipokine expression and secretion. *The Journal of Clinical Endocrinology & Metabolism* **2007,** *92* (3), 1023-33.

5. Fantuzzi, G., Adipose tissue, adipokines, and inflammation. *Journal of Allergy and Clinical Immunology* **2005,** *115* (5), 911-9; quiz 920.

6. Lefterova, M. I.; Lazar, M. A., New developments in adipogenesis. *Trends in Endocrinology & Metabolism* **2009,** *20* (3), 107-114.

7. Gil, A.; Olza, J.; Gil-Campos, M.; Gomez-Llorente, C.; Aguilera, C. M., Is adipose tissue metabolically different at different sites? *International Journal of Pediatric Obesity* **2011,** *6* (sup1), 13-20.

8. Gaggini, M.; Saponaro, C.; Gastaldelli, A., Not all fats are created equal: adipose vs. ectopic fat, implication in cardiometabolic diseases. *Hormone Molecular Biology and Clinical Investigation* **2015,** *22* (1), 7-18.

9. Fantuzzi, G.; Braunschweig, C., *Adipose tissue and adipokines in health and disease*. First ed.; Humana Press: Totowa, 2007.

10. Gesta, S.; Tseng, Y.-H.; Kahn, C. R., Developmental origin of fat: tracking obesity to its source. *Cell* **2007,** *131* (2), 242-256.

11. Choe, S. S.; Huh, J. Y.; Hwang, I. J.; Kim, J. I.; Kim, J. B., Adipose Tissue Remodeling: Its Role in Energy Metabolism and Metabolic Disorders. *Frontiers in Endocrinology* **2016,** *7*, 30.

12. Khanh, V. C.; Zulkifli, A. F.; Tokunaga, C.; Yamashita, T.; Hiramatsu, Y.; Ohneda, O., Aging impairs beige adipocyte differentiation of mesenchymal stem cells via the reduced expression of Sirtuin 1. *Biochemical and Biophysical Research Communications* **2018,** *500* (3), 682-690.

13. Paul, A., *Adipose Tissue Heterogeneity: Development and Application of Nonlinear Microscopy Methods*. Chalmers University of Technology: 2018.

14. Fruhbeck, G.; Gómez-Ambrosi, J.; Muruzábal, F. J.; Burrell, M. A., The adipocyte: a model for integration of endocrine and metabolic signaling in energy metabolism regulation. *American Journal of Physiology-Endocrinology And Metabolism* **2001,** *280* (6), E827-E847.

15. Desruisseaux, M. S.; Trujillo, M. E.; Tanowitz, H. B.; Scherer, P. E., Adipocyte, adipose tissue, and infectious disease. *Infection and immunity* **2007,** *75* (3), 1066-1078.

16. Björnheden, T.; Jakubowicz, B.; Levin, M.; Odén, B.; Edén, S.; Sjöström, L.; Lönn, M., Computerized determination of adipocyte size. *Obesity research* **2004,** *12* (1), 95-105.

17. Tsiloulis, T.; Watt, M. J., Exercise and the regulation of adipose tissue metabolism. In *Progress in molecular biology and translational science*, Elsevier: 2015; Vol. 135, pp 175-201.

18. Luu, Y.; Ozcivici, E.; Capilla, E.; Adler, B.; Chan, E.; Shroyer, K.; Rubin, J.; Judex, S.; Pessin, J. E.; Rubin, C., Development of diet-induced fatty liver disease in the aging mouse is suppressed by brief daily exposure to low-magnitude mechanical signals. *International journal of obesity* **2010,** *34* (2), 401.

19. Judex, S.; Luu, Y.; Ozcivici, E.; Adler, B.; Lublinsky, S.; Rubin, C., Quantification of adiposity in small rodents using micro-CT. *Methods* **2010,** *50* (1), 14-19.

20. Ozcivici, E.; Luu, Y. K.; Rubin, C. T.; Judex, S., Low-level vibrations retain bone marrow's osteogenic potential and augment recovery of trabecular bone during reambulation. *PloS ONE* **2010,** *5* (6), e11178.

21. Styner, M.; Thompson, W. R.; Galior, K.; Uzer, G.; Wu, X.; Kadari, S.; Case, N.; Xie, Z.; Sen, B.; Romaine, A., Bone marrow fat accumulation accelerated by high fat diet is suppressed by exercise. *Bone* **2014,** *64*, 39-46.

22. Hardouin, P.; Pansini, V.; Cortet, B., Bone marrow fat. *Joint Bone Spine* **2014,** *81* (4), 313-319.

23. Veldhuis-Vlug, A. G.; Rosen, C. J., Clinical implications of bone marrow adiposity. *Journal of internal medicine* **2018,** *283* (2), 121-139.

24. Hardouin, P.; Rharass, T.; Lucas, S., Bone marrow adipose tissue: to be or not to be a typical adipose tissue? *Frontiers in endocrinology* **2016,** *7*, 85.

25. Scheller, E. L.; Cawthorn, W. P.; Burr, A. A.; Horowitz, M. C.; MacDougald, O. A., Marrow adipose tissue: trimming the fat. *Trends in Endocrinology & Metabolism* **2016,** *27* (6), 392-403.

26. Krings, A.; Rahman, S.; Huang, S.; Lu, Y.; Czernik, P.; Lecka-Czernik, B., Bone marrow fat has brown adipose tissue characteristics, which are attenuated with aging and diabetes. *Bone* **2012,** *50* (2), 546-552.

27. Li, Q.; Wu, Y.; Kang, N., Marrow adipose tissue: its origin, function, and regulation in bone remodeling and regeneration. *Stem cells international* **2018,** *2018*.

28. de Paula, F. J. A.; Rosen, C. J., Structure and function of bone marrow adipocytes. *Comprehensive Physiology* **2011,** *8* (1), 315-349.

29. Chen, Q.; Shou, P.; Zheng, C.; Jiang, M.; Cao, G.; Yang, Q.; Cao, J.; Xie, N.; Velletri, T.; Zhang, X., Fate decision of mesenchymal stem cells: adipocytes or osteoblasts? *Cell death and differentiation* **2016,** *23* (7), 1128.

30. Muruganandan, S.; Roman, A. A.; Sinal, C. J., Role of chemerin/CMKLR1 signaling in adipogenesis and osteoblastogenesis of bone marrow stem cells. *Journal of Bone and Mineral Research* **2010,** *25* (2), 222-34.

31. Ozcivici, E.; Luu, Y. K.; Adler, B.; Qin, Y.-X.; Rubin, J.; Judex, S.; Rubin, C. T., Mechanical signals as anabolic agents in bone. *Nature Reviews Rheumatology* **2010,** *6* (1), 50.

32. Baskan, O.; Mese, G.; Ozcivici, E., Low-intensity vibrations normalize adipogenesis-induced morphological and molecular changes of adult mesenchymal stem cells. *Proceedings of the Institution of Mechanical Engineers, Part H: Journal of Engineering in Medicine* **2017,** *231* (2), 160-168.

33. Ozcivici, E.; Judex, S. In *Genetic Determinants of Musculoskeletal Adaptations to Unloading and Reloading*, 2019 9th International Conference on Recent Advances in Space Technologies (RAST), IEEE: 2019; pp 927-928.

34. Ozcivici, E.; Zhang, W.; Donahue, L. R.; Judex, S. J. B., Quantitative trait loci that modulate trabecular bone's risk of failure during unloading and reloading. **2014,** *64*, 25-32.

35. Özçivici, E., Effects of spaceflight on cells of bone marrow origin. *Turkish Journal of Hematology* **2013,** *30* (1), 1.

36. Zayzafoon, M.; Gathings, W. E.; McDonald, J. M., Modeled microgravity inhibits osteogenic differentiation of human mesenchymal stem cells and increases adipogenesis. *Endocrinology* **2004,** *145* (5), 2421-2432.

37. Justesen, J.; Stenderup, K.; Ebbesen, E.; Mosekilde, L.; Steiniche, T.; Kassem, M., Adipocyte tissue volume in bone marrow is increased with aging and in patients with osteoporosis. *Biogerontology* **2001,** *2* (3), 165-171.

38. Muruganandan, S.; Roman, A.; Sinal, C., Adipocyte differentiation of bone marrow-derived mesenchymal stem cells: cross talk with the osteoblastogenic program. *Cellular molecular life sciences* **2009,** *66* (2), 236-253.

39. Naveiras, O.; Nardi, V.; Wenzel, P. L.; Hauschka, P. V.; Fahey, F.; Daley, G. Q., Bone-marrow adipocytes as negative regulators of the haematopoietic microenvironment. *Nature* **2009,** *460* (7252), 259.

40. Zhou, B. O.; Yu, H.; Yue, R.; Zhao, Z.; Rios, J. J.; Naveiras, O.; Morrison, S. J., Bone marrow adipocytes promote the regeneration of stem cells and haematopoiesis by secreting SCF. *Nature cell biology* **2017,** *19* (8), 891.

41. Herroon, M. K.; Diedrich, J. D.; Podgorski, I., New 3D-culture approaches to study interactions of bone marrow adipocytes with metastatic prostate cancer cells. *Frontiers in endocrinology* **2016,** *7*, 84.

42. Luo, G.; He, Y.; Yu, X., Bone Marrow Adipocyte: an intimate partner with tumor cells in Bone metastasis. *Frontiers in endocrinology* **2018,** *9*, 339.

43. Greenspan, P.; Mayer, E. P.; Fowler, S. D., Nile red: a selective fluorescent stain for intracellular lipid droplets. *The Journal of cell biology* **1985,** *100* (3), 965-973.

44. Ramirez-Zacarias, J.; Castro-Munozledo, F.; Kuri-Harcuch, W., Quantitation of adipose conversion and triglycerides by staining intracytoplasmic lipids with Oil red O. *Histochemistry* **1992,** *97* (6), 493-497.

45. Martinez-Santibañez, G.; Cho, K. W.; Lumeng, C. N., Imaging white adipose tissue with confocal microscopy. In *Methods in enzymology*, Elsevier: 2014; Vol. 537, pp 17-30.

46. Varinli, H.; Osmond-McLeod, M. J.; Molloy, P. L.; Vallotton, P., LipiD-QuanT: a novel method to quantify lipid accumulation in live cells. *Journal of lipid research* **2015,** *56* (11), 2206-2216.

47. Fink, T.; Abildtrup, L.; Fogd, K.; Abdallah, B. M.; Kassem, M.; Ebbesen, P.; Zachar, V., Induction of adipocyte-like phenotype in human mesenchymal stem cells by hypoxia. *Stem cells* **2004,** *22* (7), 1346-1355.

48. De Sousa, M.; Porras, D. P.; Perry, C. G.; Seale, P.; Scimè, A., p107 is a crucial regulator for determining the adipocyte lineage fate choices of stem cells. *Stem Cells* **2014,** *32* (5), 1323-1336.

49. Ghoniem, A.-A.; Açil, Y.; Wiltfang, J.; Gierloff, M., Improved adipogenic in vitro differentiation: comparison of different adipogenic cell culture media on human fat and bone stroma cells for fat tissue engineering. *Anatomy & cell biology* **2015,** *48* (2), 85-94.

50. Majka, S. M.; Miller, H. L.; Helm, K. M.; Acosta, A. S.; Childs, C. R.; Kong, R.; Klemm, D. J., Analysis and isolation of adipocytes by flow cytometry. *Methods in Enzymology* **2014,** *537*, 281-96.

51. Boumelhem, B. B.; Assinder, S. J.; Bell-Anderson, K. S.; Fraser, S. T., Flow cytometric single cell analysis reveals heterogeneity between adipose depots. *Adipocyte* **2017,** *6* (2), 112-123.

52. Norouzi, N.; Bhakta, H. C.; Grover, W. H., Sorting cells by their density. *PloS one* **2017,** *12* (7), e0180520.

53. Hepler, C.; Vishvanath, L.; Gupta, R. K., Sorting out adipocyte precursors and their role in physiology and disease. *Genes & development* **2017,** *31* (2), 127-140.

54. Thelen, K.; Ayala-Lopez, N.; Watts, S. W.; Contreras, G. A., Expansion and Adipogenesis Induction of Adipocyte Progenitors from Perivascular Adipose Tissue Isolated by Magnetic Activated Cell Sorting. *Journal of visualized experiments: JoVE* **2017,** (124).

55. Shim, E. H.; Lee, M. S.; Lee, J. A.; Lee, H., Do In Seung Gi-Tang extract suppresses adipocyte differentiation in 3T3-L1 cells. *Molecular medicine reports* **2017,** *15* (6), 3549-3554.

56. Nakamura, M.; Decker, K.; Chosy, J.; Comella, K.; Melnik, K.; Moore, L.; Lasky, L. C.; Zborowski, M.; Chalmers, J. J., Separation of a breast cancer cell line from human blood using a quadrupole magnetic flow sorter. *Biotechnology progress* **2001,** *17* (6), 1145-1155.

57. Grover, W. H.; Bryan, A. K.; Diez-Silva, M.; Suresh, S.; Higgins, J. M.; Manalis, S. R., Measuring single-cell density. *Proceedings of the National Academy of Sciences* **2011,** *108* (27), 10992-10996.

58. Bagnaninchi, P. O.; Drummond, N., Real-time label-free monitoring of adipose-derived stem cell differentiation with electric cell-substrate impedance sensing. *Proceedings of the National Academy of Sciences* **2011**, 201018260.

59. Smus, J. P.; Moura, C. C.; McMorrow, E.; Tare, R. S.; Oreffo, R. O.; Mahajan, S., Tracking adipogenic differentiation of skeletal stem cells by label-free chemically selective imaging. *Chemical science* **2015,** *6* (12), 7089-7096.

60. Steuwe, C.; Patel, I. I.; Ul-Hasan, M.; Schreiner, A.; Boren, J.; Brindle, K. M.; Reichelt, S.; Mahajan, S., CARS based label-free assay for assessment of drugs by monitoring lipid droplets in tumour cells. *Journal of biophotonics* **2014,** *7* (11-12), 906-913.

61. Nan, X.; Cheng, J.-X.; Xie, X. S., Vibrational imaging of lipid droplets in live fibroblast cells with coherent anti-Stokes Raman scattering microscopy. *Journal of lipid research* **2003,** *44* (11), 2202-2208.

62. Wyllie, A.; Morris, R., Hormone-induced cell death. Purification ad properties of thymocytes undergoing apoptosis after glucocorticoid treatment. *The American journal of pathology* **1982,** *109* (1), 78.

63. Kumar, A. A.; Patton, M. R.; Hennek, J. W.; Lee, S. Y.; D'Alesio-Spina, G.; Yang, X.; Kanter, J.; Shevkoplyas, S. S.; Brugnara, C.; Whitesides, G. M., Density-based separation in multiphase systems provides a simple method to identify sickle cell disease. *Proc Natl Acad Sci U S A* **2014,** *111* (41), 14864-9.

64. Bryan, A. K.; Goranov, A.; Amon, A.; Manalis, S. R., Measurement of mass, density, and volume during the cell cycle of yeast. *Proceedings of the National Academy of Sciences* **2009**.

65. Kurat, C. F.; Wolinski, H.; Petschnigg, J.; Kaluarachchi, S.; Andrews, B.; Natter, K.; Kohlwein, S. D., Cdk1/Cdc28-dependent activation of the major triacylglycerol lipase Tgl4 in yeast links lipolysis to cell-cycle progression. *Molecular cell* **2009,** *33* (1), 53-63.

66. Sharpe, P. T., *Methods of cell separation*. Elsevier: 1988; Vol. 18.

67. Yamamoto, Y.; Itoh, S.; Yamauchi, Y.; Matsushita, K.; Ikeda, S.; Naruse, H.; Hayashi, M., Density gradient centrifugation for the isolation of cells of multiple lineages. *Journal of cellular biochemistry* **2015,** *116* (12), 2709-2714.

68. Björntorp, P.; Karlsson, M.; Pertoft, H.; Pettersson, P.; Sjöström, L.; Smith, U., Isolation and characterization of cells from rat adipose tissue developing into adipocytes. *Journal of lipid research* **1978,** *19* (3), 316-324.

69. Bryan, A. K.; Hecht, V. C.; Shen, W.; Payer, K.; Grover, W. H.; Manalis, S. R., Measuring single cell mass, volume, and density with dual suspended microchannel resonators. *Lab on a Chip* **2014,** *14* (3), 569-576.

70. Zhao, Y.; Lai, H. S. S.; Zhang, G.; Lee, G.-B.; Li, W. J., Rapid determination of cell mass and density using digitally controlled electric field in a microfluidic chip. *Lab on a Chip* **2014,** *14* (22), 4426-4434.

71. Zhao, Y.; Lai, H. S. S.; Zhang, G.; Lee, G.-B.; Li, W. J., Measurement of single leukemia cell's density and mass using optically induced electric field in a microfluidics chip. *Biomicrofluidics* **2015,** *9* (2), 022406.

72. Coey, J. M., *Magnetism and magnetic materials*. Cambridge university press: 2010.

73. Spain, E.; Venkatanarayanan, A.; Hashmi, M., Review of Physical Principles of Sensing and Types of Sensing Materials. *Comprehensive Materials Processing* **2014,** *13*, 5-46.

74. Mullins, C., Magnetic susceptibility of the soil and its significance in soil science–a review. *Journal of soil science* **1977,** *28* (2), 223-246.

75. Pelrine, R. E., Diamagnetic Levitation: Known since the 1930s, a simple technique for suspending objects magnetically is just now finding practical application. *American scientist* **2004,** *92* (5), 428-435.

76. Jiles, D., *Introduction to magnetism and magnetic materials*. CRC press: 2015.

77. Ahmed, J.; Ramaswamy, H. S., Applications of Magnetic Field in Food Preservation. In *Handbook of Food Preservation*, CRC Press: 2007; pp 848-859.

78. Quarterman, P.; Sun, C.; Garcia-Barriocanal, J.; Mahendra, D.; Lv, Y.; Manipatruni, S.; Nikonov, D. E.; Young, I. A.; Voyles, P. M.; Wang, J.-P., Demonstration of Ru as the 4th ferromagnetic element at room temperature. *Nature communications* **2018,** *9* (1), 2058.

79. Nigh, H. E.; Legvold, S.; Spedding, F., Magnetization and electrical resistivity of gadolinium single crystals. *Physical Review* **1963,** *132* (3), 1092.

80. Fraden, J., Handbook of modern sensors. 5th Edition ed.; Springer: 2013.

81. Zhu, T.; Cheng, R.; Liu, Y.; He, J.; Mao, L., Combining positive and negative magnetophoreses to separate particles of different magnetic properties. *Microfluidics and nanofluidics* **2014,** *17* (6), 973-982.

82. Kose, A. R.; Fischer, B.; Mao, L.; Koser, H., Label-free cellular manipulation and sorting via biocompatible ferrofluids. *Proceedings of the National Academy of Sciences* **2009,** *106* (51), 21478-21483.

83. Bwambok, D. K.; Thuo, M. M.; Atkinson, M. B.; Mirica, K. A.; Shapiro, N. D.; Whitesides, G. M., Paramagnetic ionic liquids for measurements of density using magnetic levitation. *Analytical chemistry* **2013,** *85* (17), 8442-8447.

84. Winkleman, A.; Perez-Castillejos, R.; Gudiksen, K. L.; Phillips, S. T.; Prentiss, M.; Whitesides, G. M., Density-based diamagnetic separation: devices for detecting binding events and for collecting unlabeled diamagnetic particles in paramagnetic solutions. *Analytical chemistry* **2007,** *79* (17), 6542-6550.

85. Yang, R.-J.; Hou, H.-H.; Wang, Y.-N.; Fu, L.-M., Micro-magnetofluidics in microfluidic systems: A review. *Sensors and Actuators B: Chemical* **2016,** *224*, 1-15.

86. Huang, S.; Yong-Qing, H.; Feng, J., Advances of particles/cells magnetic manipulation in microfluidic chips. *Chinese Journal of Analytical Chemistry* **2017,** *45* (8), 1238-1246.

87. Zhao, W.; Cheng, R.; Miller, J. R.; Mao, L., Label-Free Microfluidic Manipulation of Particles and Cells in Magnetic Liquids. *Advanced functional materials* **2016,** *26* (22), 3916-3932.

88. Zhao, W.; Cheng, R.; Lim, S. H.; Miller, J. R.; Zhang, W.; Tang, W.; Xie, J.; Mao, L., Biocompatible and label-free separation of cancer cells from cell culture lines from white blood cells in ferrofluids. *Lab on a Chip* **2017,** *17* (13), 2243-2255.

89. Mirica, K. A.; Shevkoplyas, S. S.; Phillips, S. T.; Gupta, M.; Whitesides, G. M., Measuring densities of solids and liquids using magnetic levitation: fundamentals. *Journal of the American Chemical Society* **2009,** *131* (29), 10049-10058.

90. Rodríguez-Villarreal, A. I.; Tarn, M. D.; Madden, L. A.; Lutz, J. B.; Greenman, J.; Samitier, J.; Pamme, N., Flow focussing of particles and cells based on their intrinsic properties using a simple diamagnetic repulsion setup. *Lab on a Chip* **2011,** *11* (7), 1240-1248.

91. Kirchin, M. A.; Runge, V. M., Contrast agents for magnetic resonance imaging: safety update. *Topics in Magnetic Resonance Imaging* **2003,** *14* (5), 426-435.

92. Cheng, K. T., Gadobutrol. In *Molecular Imaging and Contrast Agent Database (MICAD)[Internet]*, National Center for Biotechnology Information (US): 2007.

93. Rogosnitzky, M.; Branch, S., Gadolinium-based contrast agent toxicity: a review of known and proposed mechanisms. *Biometals* **2016,** *29* (3), 365-376.

94. Knowlton, S.; Yu, C. H.; Jain, N.; Ghiran, I. C.; Tasoglu, S., Smart-phone based magnetic levitation for measuring densities. *PLoS One* **2015,** *10* (8), e0134400.

95. Sarigil, O.; Anil, M.; Yilmaz, E.; Mese, G.; Tekin, H. C.; Ozcivici, E., Label-free density-based detection of adipocytes of bone marrow origin using magnetic levitation. *Analyst* **2019**.

96. Ge, S.; Wang, Y.; Deshler, N. J.; Preston, D. J.; Whitesides, G. M., High-Throughput Density Measurement Using Magnetic Levitation. *Journal of the American Chemical Society* **2018,** *140* (24), 7510-7518.

97. Anil-Inevi, M.; Yilmaz, E.; Sarigil, O.; Tekin, H. C.; Ozcivici, E., Single Cell Densitometry and Weightlessness Culture of Mesenchymal Stem Cells Using Magnetic Levitation. Springer: 2019.

98. Trog, S.; El-Khatib, A. H.; Beck, S.; Makowski, M. R.; Jakubowski, N.; Linscheid, M. W., Complementarity of molecular and elemental mass spectrometric imaging of Gadovist™ in mouse tissues. *Analytical bioanalytical chemistry* **2019,** *411* (3), 629-637.

99. Winkleman, A.; Gudiksen, K. L.; Ryan, D.; Whitesides, G. M.; Greenfield, D.; Prentiss, M., A magnetic trap for living cells suspended in a paramagnetic buffer. *Applied Physics Letters* **2004,** *85* (12), 2411-2413.

100. Coleman, C. B.; Gonzalez-Villalobos, R. A.; Allen, P. L.; Johanson, K.; Guevorkian, K.; Valles, J. M.; Hammond, T. G., Diamagnetic levitation changes growth, cell cycle, and gene expression of Saccharomyces cerevisiae. *Biotechnology and Bioengineering* **2007,** *98* (4), 854-63.

101. Simon, M. D.; Geim, A. K., Diamagnetic levitation: Flying frogs and floating magnets (invited). *Journal of Applied Physics* **2000,** *87* (9), 6200-6204.

102. Beaugnon, E.; Tournier, R., Levitation of water and organic substances in high static magnetic fields. *Journal de Physique III* **1991,** *1* (8), 1423-1428.

103. Hirota, N.; Kurashige, M.; Iwasaka, M.; Ikehata, M.; Uetake, H.; Takayama, T.; Nakamura, H.; Ikezoe, Y.; Ueno, S.; Kitazawa, K., Magneto-Archimedes separation and its application to the separation of biological materials. *Physica B: Condensed Matter* **2004,** *346*, 267-271.

104. Russell, A. P.; Evans, C. H.; Westcott, V. C., Measurement of the susceptibility of paramagnetically labeled cells with paramagnetic solutions. *Analytical biochemistry* **1987,** *164* (1), 181-189.

105. Yaman, S.; Anil-Inevi, M.; Ozcivici, E.; Tekin, H. C., Magnetic Force-Based Microfluidic Techniques for Cellular and Tissue Bioengineering. *Front Bioeng Biotechnol* **2018,** *6*, 192.

106. Hejazian, M.; Nguyen, N.-T., Negative magnetophoresis in diluted ferrofluid flow. *Lab on a Chip* **2015,** *15* (14), 2998-3005.

107. Souza, G. R.; Molina, J. R.; Raphael, R. M.; Ozawa, M. G.; Stark, D. J.; Levin, C. S.; Bronk, L. F.; Ananta, J. S.; Mandelin, J.; Georgescu, M.-M., Three-dimensional tissue culture based on magnetic cell levitation. *Nature nanotechnology* **2010,** *5* (4), 291.

108. Sarigil, O.; Anil-Inevi, M.; Yilmaz, E.; Cagan, M.; Mese, G.; Tekin, H. C.; Ozcivici, E. In *Application of Magnetic Levitation Induced Weightlessness to Detect Cell Lineage*, 2019 9th International Conference on Recent Advances in Space Technologies (RAST), IEEE: 2019; pp 933-935.

109. Anil-Inevi, M.; Yaman, S.; Yildiz, A. A.; Mese, G.; Yalcin-Ozuysal, O.; Tekin, H. C.; Ozcivici, E., Biofabrication of in situ Self Assembled 3D Cell Cultures in a Weightlessness Environment Generated using Magnetic Levitation. *Scientific Reports* **2018,** *8* (1), 7239.

110. Parfenov, V. A.; Koudan, E. V.; Bulanova, E. A.; Karalkin, P. A.; Pereira, F. D.; Norkin, N. E.; Knyazeva, A. D.; Gryadunova, A. A.; Petrov, O. F.; Vasiliev, M. M., Scaffold-free, label-free and nozzle-free biofabrication technology using magnetic levitational assembly. *Biofabrication* **2018,** *10* (3), 034104.

111. Türker, E.; Demirçak, N.; Arslan-Yildiz, A., Scaffold-free three-dimensional cell culturing using magnetic levitation. *Biomaterials Science* **2018,** *6* (7), 1745-1753.

112. Anil-Inevi, M.; Yalcin-Ozuysal, O.; Sarigil, O.; Mese, G.; Ozcivici, E.; Yaman, S.; Tekin, H. C. In *Biofabrication of Cellular Structures Using Weightlessness as a Biotechnological Tool*, 2019 9th International Conference on Recent Advances in Space Technologies (RAST), IEEE: 2019; pp 929-931.

113. Qian, A. R.; Yin, D. C.; Yang, P. F.; Lv, Y.; Tian, Z. C.; Shang, P., Application of Diamagnetic Levitation Technology in Biological Sciences Research. *IEEE Transactions on Applied Superconductivity* **2013,** *23* (1), 3600305-3600305.

114. Herranz, R.; Larkin, O. J.; Dijkstra, C. E.; Hill, R. J.; Anthony, P.; Davey, M. R.; Eaves, L.; van Loon, J. J.; Medina, F. J.; Marco, R., Microgravity simulation by diamagnetic levitation: effects of a strong gradient magnetic field on the transcriptional profile of Drosophila melanogaster. *BMC genomics* **2012,** *13* (1), 52.

115. Coleman, C. B.; Allen, P. L.; Valles, J. M.; Hammond, T. G., Transcriptional regulation of changes in growth, cell cycle, and gene expression of Saccharomyces cerevisiae due to changes in buoyancy. *Biotechnol Bioeng* **2008,** *100* (2), 334-43.

116. Zhu, T.; Cheng, R.; Lee, S. A.; Rajaraman, E.; Eiteman, M. A.; Querec, T. D.; Unger, E. R.; Mao, L., Continuous-flow ferrohydrodynamic sorting of particles and cells in microfluidic devices. *Microfluidics and nanofluidics* **2012,** *13* (4), 645-654.

117. Akiyama, Y.; Morishima, K., Label-free cell aggregate formation based on the magneto-Archimedes effect. *Applied Physics Letters* **2011,** *98* (16), 163702.

118. Ge, S.; Whitesides, G. M., "Axial" Magnetic Levitation Using Ring Magnets Enables Simple Density-Based Analysis, Separation, and Manipulation. *Analytical Chemistry* **2018,** *90* (20), 12239-12245.

119. Zhang, C.; Zhao, P.; Gu, F.; Xie, J.; Xia, N.; He, Y.; Fu, J., Single-Ring Magnetic Levitation Configuration for Object Manipulation and Density-Based Measurement. *Analytical Chemistry* **2018,** *90* (15), 9226-9233.

120. Gao, Q.-H.; Li, W.-B.; Zou, H.-X.; Yan, H.; Peng, Z.-K.; Meng, G.; Zhang, W.-M., A centrifugal magnetic levitation approach for high-reliability density measurement. *Sensors and Actuators B: Chemical* **2019**.

121. Demiray, L.; Özçivici, E., Bone marrow stem cells adapt to low-magnitude vibrations by altering their cytoskeleton during quiescence and osteogenesis. *Turkish Journal of Biology* **2015,** *39* (1), 88-97.

122. Durmus, N. G.; Tekin, H. C.; Guven, S.; Sridhar, K.; Arslan Yildiz, A.; Calibasi, G.; Ghiran, I.; Davis, R. W.; Steinmetz, L. M.; Demirci, U., Magnetic levitation of single cells. *Proceedings of the National Academy of Sciences* **2015,** *112* (28), E3661-8.

123. Yenilmez, B.; Knowlton, S.; Yu, C. H.; Heeney, M. M.; Tasoglu, S., Label-free sickle cell disease diagnosis using a low-cost, handheld platform. *Advanced Materials Technologies* **2016,** *1* (5), 1600100.

124. Yenilmez, B.; Knowlton, S.; Tasoglu, S., Self-contained handheld magnetic platform for point of care cytometry in biological samples. *Advanced Materials Technologies* **2016,** *1* (9), 1600144.

125. Felton, E. J.; Velasquez, A.; Lu, S.; Murphy, R. O.; ElKhal, A.; Mazor, O.; Gorelik, P.; Sharda, A.; Ghiran, I. C., Detection and quantification of subtle changes in red blood cell density using a cell phone. *Lab on a Chip* **2016,** *16* (17), 3286-3295.

126. Knowlton, S.; Sencan, I.; Aytar, Y.; Khoory, J.; Heeney, M.; Ghiran, I.; Tasoglu, S., Sickle cell detection using a smartphone. *Scientific reports* **2015,** *5*, 15022.

127. Bellin, M.-F.; Van Der Molen, A. J., Extracellular gadolinium-based contrast media: an overview. *European journal of radiology* **2008,** *66* (2), 160-167.

128. Guo, B. J.; Yang, Z. L.; Zhang, L. J., Gadolinium Deposition in Brain: Current Scientific Evidence and Future Perspectives. *Frontiers in molecular neuroscience* **2018,** *11*.

129. Fielding, P. E.; Fielding, C. J., Dynamics of lipoprotein transport in the human circulatory system. In *New Comprehensive Biochemistry*, Elsevier: 2002; Vol. 36, pp 527-552.

130. Walther, T. C.; Farese Jr, R. V., Lipid droplets and cellular lipid metabolism. *Annual review of biochemistry* **2012,** *81*, 687-714.

131. Loo, L.-H.; Lin, H.-J.; Singh, D. K.; Lyons, K. M.; Altschuler, S. J.; Wu, L. F., Heterogeneity in the physiological states and pharmacological responses of differentiating 3T3-L1 preadipocytes. *The Journal of cell biology* **2009,** *187* (3), 375-384.

132. Le, T. T.; Cheng, J.-X., Single-cell profiling reveals the origin of phenotypic variability in adipogenesis. *PLoS One* **2009,** *4* (4), e5189.

133. Herms, A.; Bosch, M.; Ariotti, N.; Reddy, B. J.; Fajardo, A.; Fernández-Vidal, A.; Alvarez-Guaita, A.; Fernández-Rojo, M. A.; Rentero, C.; Tebar, F., Cell-to-cell heterogeneity in lipid droplets suggests a mechanism to reduce lipotoxicity. *Current Biology* **2013,** *23* (15), 1489-1496.

134. Juopperi, T. A.; Schuler, W.; Yuan, X.; Collector, M. I.; Dang, C. V.; Sharkis, S. J., Isolation of bone marrow–derived stem cells using density-gradient separation. *Experimental hematology* **2007,** *35* (2), 335-341.

135. Farvid, M.; Ng, T.; Chan, D.; Barrett, P.; Watts, G., Association of adiponectin and resistin with adipose tissue compartments, insulin resistance and dyslipidaemia. *Diabetes, obesity and metabolism* **2005,** *7* (4), 406-413.

136. Martin, A.; Daniel, M.; Drinkwater, D.; Clarys, J., Adipose tissue density, estimated adipose lipid fraction and whole body adiposity in male cadavers. *International journal of obesity and related metabolic disorders: journal of the International Association for the Study of Obesity* **1994,** *18* (2), 79-83.

137. Jo, J.; Gavrilova, O.; Pack, S.; Jou, W.; Mullen, S.; Sumner, A. E.; Cushman, S. W.; Periwal, V., Hypertrophy and/or Hyperplasia: Dynamics of Adipose Tissue Growth. *PLoS Comput Biol* **2009,** *5* (3), e1000324.

138. Skurk, T.; Alberti-Huber, C.; Herder, C.; Hauner, H., Relationship between adipocyte size and adipokine expression and secretion. *The Journal of Clinical Endocrinology and Metabolism* **2007,** *92* (3), 1023-1033.

139. Kubitschek, H. E., Buoyant density variation during the cell cycle in microorganisms. *CRC Critical reviews in microbiology* **1987,** *14* (1), 73-97.

140. Baldwin, W. W.; Myer, R.; Powell, N.; Anderson, E.; Koch, A. L., Buoyant density of Escherichia coli is determined solely by the osmolarity of the culture medium. *Archives of microbiology* **1995,** *164* (2), 155-157.

141. Baldwin, W. W.; Kubitschek, H. E., Evidence for osmoregulation of cell growth and buoyant density in Escherichia coli. *Journal of bacteriology* **1984,** *159* (1), 393-394.